

Synchronization thresholds of coupled self-excited nonidentical pendula suspended on the vertically displacing beam

Marcin Kapitaniak^{1,2}, Piotr Brzeski¹, Krzysztof Czolczynski¹, Przemysław Perlikowski¹, Andrzej Stefanski¹, and Tomasz Kapitaniak^{1*}

¹*Division of Dynamics, Technical University of Lodz, Stefanowskiego 1/15, 90-924 Lodz, Poland*

²*Centre for Applied Dynamics Research, School of Engineering, University of Aberdeen AB24 3UE, Aberdeen, Scotland*

PACS: 45.40.-f, 05.45.-a

Keywords: synchronization, bifurcations, self-excited systems

Abstract: The synchronization of a number of self-excited nonidentical pendula (with the same masses and different lengths) hanging on the same beam which can move vertically has been investigated. We identify different synchronous configurations and investigate their stability. An approximate analytical analysis of the energy balance allows to derive the synchronization conditions, phase difference between the pendula and explains the observed types of synchronizations. We give evidence of two thresholds (in a number of pendula and differences in lengths) after which the synchronization is not observed. It has been shown that for more than three pendula with sufficiently large differences in the lengths the synchronization is not observed and the pendula perform quasi-periodic oscillations. Our results are robust as they exist for the wide set of system parameters.

1. Introduction

Recent investigations have shown that the coupled systems have great potential in a large amount of application areas ranging from physics and engineering to economy and biology [1-5 and ref. within]. The main interest in these studies is concentrated on the phenomenon of synchronization. The phenomenon of mutual synchronization offers the most fundamental example of emergent behavior. The synchronization of pedestrians on Millennium bridge [6-12] was a very spectacular example in engineering.

Synchronization means adjustment of rhythms of self-sustained periodic oscillators due to their weak interaction; this adjustment can be described in terms of phase locking and frequency entrainment [1,5]. Modern concept considers also the synchronization of rotators (rotating pendula) and chaotic systems; in the latter case one distinguishes between different forms of synchronization: complete/identical, phase, generalized, etc.[1,13,14 and ref. within]. The synchronization phenomena in large ensembles of coupled systems often manifest themselves as collective coherent regimes appearing via non-equilibrium phase transitions.

The history of synchronization goes back to 17th century when Ch. Huygens reported his observation of synchronization of two pendulum clocks which he had invented shortly before. "It is quite worth noting that when we suspended two clocks so constructed from two hooks imbedded in the same wooden beam, the motions of each pendulum in opposite swings were so much in agreement that they never receded the least bit from each other and the sound of each was always heard simultaneously. Further, if this agreement was disturbed by some interference, it reestablished itself in a short time. For a long time I was amazed at this

unexpected result, but after a careful examination finally found that the cause of this is due to the motion of the beam, even though this is hardly perceptible" [15,16]. Another important observation of synchrony of organ pipes was described by Lord Reyleigh in his "Theory of Sound". Being probably the oldest scientifically studied nonlinear effect, synchronization was understood only in 1920-ies when B. van der Pol systematically studied synchronization of triode electronic generators [17].

Huygens' experiment has attracted increasing attention from different research groups [18-30] and stimulated even more studies of the dynamics of coupled pendula [30-38]. In the previous papers [26-30] we studied a synchronization problem for n pendulum clocks hanging from an elastically fixed horizontal beam. It was assumed that each pendulum performs periodic motion which starts from different initial conditions. We showed that after a transient different types of synchronization between pendula can be observed. The first type is in-phase complete synchronization in which all pendula behave identically. In the second type one can identify the groups (clusters) of synchronized pendula. We showed that only configurations of three and five clusters are possible and derive algebraic equations for the phase difference between the pendula in different clusters.

In this paper we consider the case of n nonidentical self-excited pendula (pendula have the same masses but different lengths) hanging from the same beam. The oscillations of each pendulum are self-excited by van-der Pol's type of damping. Contrary to the previously considered cases [18-30], we assume that the beam can oscillate not in the horizontal but in vertical direction. We identify two kinds of synchronous configurations. Configurations of the first kind (almost complete synchronization during which all pendula oscillate in the same way, almost antiphase synchronization of two clusters of completely synchronized pendula) are characterized by the large resultant force with which the pendula act on the beam. The configurations of the second kind (phase synchronization with the constant phase shifts between the pendula) exist for up to $n=3$ pendula and are characterized by the small value of the resultant force with which pendula act on the beam. As the result the beam oscillates with a small amplitude. We give evidence of two thresholds (in a number of pendula and differences in lengths) after which the synchronization is not observed. For the system with a large number of pendula and sufficiently large differences in lengths we mainly observe quasi-periodic oscillations.

The paper is organized as follows. In Sec.2 we present our theoretical model which describes the dynamics of n coupled non-identical pendula. Approximate analytical conditions for the synchronization are given in Sec. 3. Here we derive equations for the estimation of the phase shifts between the pendula. Section 4 presents the results of our numerical studies. We show typical examples of stable phase synchronization configurations and discuss energy balances associated with them. Finally, we discuss why other configurations are not possible and summarize our results in Sec. 4.

2. The system

The analyzed system is shown in Figure 1. It consists of a rigid beam and a number of pendula suspended on it. The beam of mass M can displace only vertically (it has one degree of freedom); it is connected with the frame by a massless linear spring of stiffness coefficient K_Y and a viscous damper of damping coefficient C_Y . The displacement of the beam is described by coordinate Y . The pendula have the form of mathematical pendula of lengths L_i and masses M_i . The motion of the pendula is described by angles φ_i and is self-excited by van der Pol's type of damping (not shown in Figure 1) given by momentum (torque) $C_{\varphi_i} \frac{d\varphi_i}{dt} (1 - C_{VDPi} \varphi_i^2)$, where C_{φ_i} and C_{VDPi} are constant.

The equation of motion for the above-described system can be written as follows:

$$M_i L_i^2 \frac{d^2 \varphi_i}{dt^2} - M_i L_i \frac{d^2 Y}{dt^2} \sin \varphi_i + C_{\varphi_i} (1.0 - C_{VDP_i} \varphi_i^2) \frac{d \varphi_i}{dt} + M_i L_i g \sin \varphi_i = 0.0, \quad i = 1 \dots n \quad (1)$$

$$\left(M_B + \sum_{i=1}^n M_i \right) \frac{d^2 Y}{dt^2} + C_Y \frac{dY}{dt} + K_Y Y = \sum_{i=1}^n M_i L_i \left(\frac{d^2 \varphi_i}{dt^2} \sin \varphi_i + \left(\frac{d \varphi_i}{dt} \right)^2 \cos \varphi_i \right). \quad (2)$$

Considering mass M_1 and length L_1 of the first pendulum and the gravitational acceleration g as the reference quantities, the dimensional eqs (1,2) can be rewritten in a dimensionless form as:

$$m_i l_i^2 \ddot{\varphi}_i - m_i l_i \ddot{y} \sin \varphi_i + c_{\varphi_i} (1.0 - c_{VDP_i} \varphi_i^2) \dot{\varphi}_i + m_i l_i \sin \varphi_i = 0.0, \quad i = 1 \dots n \quad (3)$$

$$\left(m_B + \sum_{i=1}^n m_i \right) \ddot{y} + c_y \dot{y} + k_y y = \sum_{i=1}^n m_i l_i (\ddot{\varphi}_i \sin \varphi_i + \dot{\varphi}_i^2 \cos \varphi_i) \quad (4)$$

The relationships between the dimensional quantities of eqs (1) and (2) and the dimensionless

quantities of eqs (3) and (4) are as follow: $m_i = \frac{M_i}{M_1}$ (dimensionless mass of the i th pendulum),

$l_i = \frac{L_i}{L_1}$ (dimensionless length of the i th pendulum), $\tau = \alpha t$ (dimensionless time), $\alpha = \sqrt{\frac{g}{L_1}}$,

$y = \frac{Y}{L_1}$ (dimensionless displacement of the beam M), $c_{\varphi_i} = \frac{C_{\varphi_i} \sqrt{L_1}}{M_1 L_1^2 \sqrt{g}}$, $c_{VDP_i} = C_{VDP_i}$, $m_B = \frac{M_B}{M_1}$

$c_y = \frac{C_Y \sqrt{L_1}}{M_1 \sqrt{g}}$, $k_y = \frac{K_Y L_1}{M_1 g}$, symbols $\ddot{}$ and $\dot{}$ denote respectively $\frac{d^2}{d\tau^2}$ and $\frac{d}{d\tau}$.

Multiplying eq. (3) by the i -th pendulum angular velocity $\dot{\varphi}_i$ one gets

$$m_i l_i^2 \ddot{\varphi}_i \dot{\varphi}_i + m_i l_i \dot{\varphi}_i \sin \varphi_i = -c_{\varphi_i} \dot{\varphi}_i^2 + c_{\varphi_i} c_{VDP_i} \varphi_i^2 \dot{\varphi}_i^2 + m_i l_i \ddot{y} \sin \varphi_i \dot{\varphi}_i, \quad i = 1 \dots n. \quad (5)$$

When the motion of the pendula and the beam is periodic, after the integration of eq.(5) we obtain the energy balance of the i -th pendulum:

$$\begin{aligned} & \int_0^T m_i l_i^2 \ddot{\varphi}_i \dot{\varphi}_i d\tau + \int_0^T m_i l_i \dot{\varphi}_i \sin \varphi_i d\tau = \\ & = -\int_0^T c_{\varphi_i} \dot{\varphi}_i^2 d\tau + \int_0^T c_{\varphi_i} c_{VDP_i} \varphi_i^2 \dot{\varphi}_i^2 d\tau + \int_0^T m_i l_i \ddot{y} \sin \varphi_i \dot{\varphi}_i d\tau, \quad i = 1 \dots n \end{aligned} \quad (6)$$

Left hand side of eq. (6) represents the increase of the total energy of i -th pendulum. When the motion of the whole system (the pendula and the beam) is periodic this increase is equal to zero:

$$\int_0^T m_i l_i^2 \ddot{\varphi}_i \dot{\varphi}_i d\tau + \int_0^T m_i l_i \dot{\varphi}_i \sin \varphi_i d\tau = 0, \quad i = 1, \dots, n. \quad (7)$$

The first and the second components of the right hand side of eq.(6) represent respectively the energy supplied

$$W_i^{SELF} = -\int_0^T c_{\varphi_i} \dot{\varphi}_i^2 d\tau, \quad i = 1, \dots, n. \quad (8)$$

and the energy dissipated by van der Pol's dampers:

$$W_i^{VDP} = -\int_0^T c_{\phi_i} c_{VDPi} \dot{\phi}_i^2 dt, \quad i = 1, \dots, n. \quad (9)$$

The last component of the right hand side of eq.(6) :

$$W_i^{SYN} = -\int_0^T m_i l_i \ddot{y} \sin \phi_i \dot{\phi}_i d\tau, \quad i = 1, \dots, n. \quad (10)$$

represents the energy transferred by i -th pendulum to the beam (when $W_i^{SYN} > 0$) or the energy transferred from the beam to the i -th pendulum (when $W_i^{SYN} < 0$).

Substituting eqs.(7-10) into eq.(6) one gets the following energy balances of pendula

$$W_i^{SELF} = W_i^{VDP} + W_i^{SYN}, \quad i = 1, \dots, n. \quad (11)$$

Multiplying eq. (4) by the i -th pendulum angular velocity $\dot{\phi}_i$ one gets

$$\left(m_B + \sum_{i=1}^n m_i \right) \ddot{y} + c_y \dot{y}^2 + k_y y \dot{y} = \sum_{i=1}^n m_i l_i \dot{y} (\ddot{\phi}_i \sin \phi_i + \dot{\phi}_i^2 \cos \phi_i) \quad (12)$$

When the motion of the pendula and the beam is periodic, after the integration of eq.(12) we obtain the energy balance of the beam:

$$\int_0^T \left(m_B + \sum_{i=1}^n m_i \right) \ddot{y} \dot{y} d\tau + \int_0^T k_y y \dot{y} d\tau = -\int_0^T c_y \dot{y}^2 d\tau + \int_0^T \left(\sum_{i=1}^n m_i l_i (\ddot{\phi}_i \sin \phi_i + \dot{\phi}_i^2 \cos \phi_i) \right) \dot{y} d\tau. \quad (13)$$

Left hand side of eq. (13)

$$\int_0^T \left(m_B + \sum_{i=1}^n m_i \right) \ddot{y} \dot{y} d\tau + \int_0^T k_y y \dot{y} d\tau = 0 \quad (14)$$

represents the increase of the total energy of the beam. For the periodic motion of the system this increase is equal to zero. The first component of the right hand side of eq.(13)

$$W_{beam} = \int_0^T c_y \dot{y}^2 d\tau \quad (15)$$

represents the energy dissipated by the viscous damper c_y . The second component denoted by:

$$\sum_{i=1}^{i=n} (-W_i^{SYN}) = \int_0^T \left(\sum_{i=1}^n m_i l_i (\ddot{\phi}_i \sin \phi_i + \dot{\phi}_i^2 \cos \phi_i) \right) \dot{y} d\tau \quad (16)$$

represents the energy supplied to the beam by n pendula during one period of oscillations (the sum of works performed by the forces with which n pendula act on the beam). Substituting eq.(14-16) into eq.(13) one gets the formula

$$W_{beam} = \sum_{i=1}^{i=n} (W_i^{SYN}), \quad (17)$$

which gives the energy balance of the beam.

3. Synchronous configurations in the system with identical pendula

To explain how the synchronization can be achieved in the system of Figure 1 first consider the case of identical pendula and nonmovable beam. In this case all pendula have the same period of oscillations (the pendula have the same masses and lengths). The oscillations of the pendula are initiated by the non-zero initial conditions and the pendula's evolutions tend to the limit cycles (representing periodic oscillations). The pendula are not coupled and the phase angles between their oscillations have fixed values, depending on initial conditions. Any perturbation of the pendula oscillations results in the changes of these angles.

When the beam can move vertically, the oscillations of the beam excited by the forces with which pendula act on it, cause the changes of the phase shifts between the pendula's displacements and differentiate the periods of their oscillations. When after transient time, all pendula have the same period of oscillations and there are constant phase shifts between the pendula's displacements, we can say that the pendula achieve synchronization. The state of synchronization is achieved when the motion of the system is periodic and there are constant phase shifts between the pendula displacements. The values of the phase shifts characterize the synchronous configuration and are independent of the initial conditions (unless the initial conditions belong to the basin of attraction of the particular configuration).

In the considered system we identify two basic kinds of synchronization. In the first one each pendulum transmits positive energy W_i^{SYN} to the beam. The sum of these energies, i.e., the energy W_{beam} is dissipated by beam damper c_y , as given by eq. (17). In this synchronous state the total force with which the pendula act on the beam is large and the beam oscillates with a large amplitude. This results in either complete or antiphase-synchronization. In the second kind, some pendula provide the energy to others through the beam. For the pendula which transmit energy to the beam, the amplitudes of their oscillations decrease (are smaller than in the case when the beam is at rest) and for the pendula which take energy from the beam, the amplitudes of their oscillations increase (are larger than in the case when the beam is at rest) and for these pendula the energy W_i^{SYN} is negative. In this synchronous state, the total force with which the pendula act on the beam is small (close to zero) and so is the amplitude of the beam oscillations (e.g. 60° , 120° and 90° - synchronization).

If the amplitudes of the pendula's oscillations are small, they can be described by the harmonic functions:

$$\varphi_i = \Phi_i \sin(\tau + \beta_i) \quad (18)$$

(note that the frequency of pendulum free oscillations equals 1 in the dimensionless notation),

and thus the functions describing velocity and acceleration are as follow:

$$\begin{aligned} \dot{\varphi}_i &= \Phi_i \cos(\tau + \beta_i) \\ \ddot{\varphi}_i &= -\Phi_i \sin(\tau + \beta_i) \end{aligned} \quad (19)$$

After the substitution of eqs. (18) and (19) into the beam motion equation (4), one obtains the expression for the total force with which the pendula act on the beam:

$$F = \sum_{i=1}^n (m_i l_i \Phi_i^2 \cos(2\tau + 2\beta_i)). \quad (20)$$

For a sufficiently small value of damping coefficient c_y , the oscillations of the beam are described as follows

$$y = \sum_{i=1}^n (Y_i \cos(2\tau + 2\beta_i)). \quad (21)$$

i.e., by the harmonic function with a period twice shorter than the period of the pendula. For the identical pendula and the small value of energy W_{beam} dissipated by the beam damper, the values of all energies W_i^{SYN} are equal to zero. Substituting eqs (18) and (21) into eq. (10) and equalizing energy W_i^{SYN} to zero one concludes that in the state of synchronization the phase angles β_i have to fulfill one of the following conditions:

$$\sin(2\beta_i - 2\beta_k) = 0.0, \quad i = 1, \dots, n, \quad k = 1, \dots, n. \quad (22)$$

(the first kind of synchronization) or

$$\sum_{i=1}^n \cos 2\beta_i = 0, \quad \sum_{i=1}^n \sin 2\beta_i = 0. \quad (23)$$

(the second kind of synchronization).

The phase angles $\beta_1, \beta_2, \dots, \beta_n$ calculated from eq. (22) or (23) define the phase shifts between the pendula's displacements in different synchronous configurations. For two pendula ($n=2$) and $\beta_1=0.0^\circ$ (the value of one angle can be arbitrarily chosen), the condition given by eq.(22) is fulfilled by the following angles: (i) $\beta_1 = \beta_2 = 0.0^\circ$, i.e., complete synchronization, (ii) $\beta_1 = 0.0^\circ, \beta_2 = 180.0^\circ$, i.e., antiphase synchronization, (iii) $\beta_1=0.0^\circ, \beta_2=90.0^\circ$, i.e. 90° -synchronization. In the case of 90° -synchronization the angle $\beta_2=90^\circ$ additionally fulfills eq.(23) which for $n=2$ pendula has the following form:

$$\begin{aligned} 1.0 + \cos 2\beta_2 &= 0, \\ \sin 2\beta_2 &= 0. \end{aligned} \tag{24}$$

For three pendula ($n=3$) and $\beta_1=0.0^\circ$, eq. (22) is fulfilled by the following angles: (i) $\beta_1=\beta_2=\beta_3=0.0^\circ$, i.e., complete synchronization; (ii) $\beta_1=0.0^\circ, \beta_2=\beta_3=180.0^\circ$, i.e., antiphase synchronization of one pendulum and a cluster of two pendula in the state of complete synchronization. Eq. (23) which has the following form

$$\begin{aligned} 1.0 + \cos 2\beta_2 + \cos 2\beta_3 &= 0, \\ \sin 2\beta_2 + \sin 2\beta_3 &= 0. \end{aligned} \tag{25}$$

is fulfilled by the angles: (iii) $\beta_1=0.0^\circ, \beta_2=60^\circ, \beta_3=120.0^\circ - 60^\circ$ - phase synchronization; (iv) $\beta_1=0.0^\circ, \beta_2=120^\circ, \beta_3= 240.0^\circ$, i.e., 120° -phase synchronization.

Note that for the phase angles fulfilling eq.(23), the total force with which the pendula act on the beam given by eq.(20) is equal to zero and the beam is at rest. This situation occurs for 90° phase synchronization of two pendula and 60° - and 120° - phase synchronization of three pendula. In all other synchronous states the total force is not equal to zero and the beam oscillates with the frequency twice larger than the frequency of the pendula's oscillations.

4. Numerical simulations

We consider the examples of synchronous configurations and the maps showing the dependence of the type of the synchronous state on the initial conditions and system parameters. Our results have been obtained by numerical integration (by 4th order Runge-Kutta method) of eqs. (3) and (4).

The decisive factor (in addition to the parameters of the system) which defines the type of the achieved synchronous configuration is the set of initial conditions. To describe the initial state of the studied system one requires the determination of $2(1+n)$ initial conditions, therefore, already in the simplest case of two pendula the set of initial conditions is 6-dimensional. To reduce the dimension of this set we impose certain limitations. We assume that the numerical simulations start from the state in which the pendula suspended on the nonmovable beam perform the oscillations described by eq.(18). For the initial time $t=0$, the state of the i -th pendulum is described by the initial value of φ_{i0} pendulum displacement and initial velocity $\dot{\varphi}_{i0}$:

$$\begin{aligned} \varphi_{i0} &= \Phi \sin \beta_{i0}, \\ \dot{\varphi}_{i0} &= \alpha \Phi \cos \beta_{i0}. \end{aligned} \tag{26}$$

Under this assumption the initial state of the i -th pendulum is fully described by one value β_{i0} . We consider the following initial conditions of the beam $y_0=0, \dot{y}_0 = 0$.

We consider the following values of the system parameters: $c_{\varphi i}=-0.01, c_{VDPi}=60.0$ (for these values the amplitude of the pendula oscillations when the beam is at rest is equal to $\Phi_i=0.25 \approx 15^\circ$), $m_b=2.0, k_y=10.0$. The damping coefficient of the beam c_y depends on the

number of pendula and the assumed logarithmic decrease of damping $\Delta=\ln 1.2$ (the oscillator with stiffness coefficient k_y and mass equal to the total mass of the beam and pendula m_b+n). The relations between the lengths of the pendula are given in the following examples.

4.1. Synchronization of two identical pendula

Figure 2(a-d) presents the examples of the synchronous configurations predicted in Sec. 3. The displacements of the pendula and the displacement of the beam (10 times enlarged) are shown versus time (the unit of time on the horizontal axis is the number of pendula's periods when the beam is at rest N). In Figure 2(a) one observes the **complete synchronization**, during which the pendula's displacements are identical ($\varphi_1=\varphi_2$) and the beam oscillates with the frequency twice larger than the pendula's frequency. Figure 2(b) presents the **antiphase synchronization**, during which the pendula's displacements fulfill the relation $\varphi_1=-\varphi_2$ and the beam oscillates with the frequency twice larger than the pendula's frequency. Note that the time series of the beam displacement is the same as in the case of complete synchronization. Figure 2(c) shows **90°-1/2 synchronization**, during which the phase shift between the pendula's displacements is equal to 90° and the main (the second) harmonic of the beam oscillations is equal to zero, i.e., the beam is practically at rest. Symbol „1/2” denotes that the displacement φ_1 of pendulum 1 is phase delayed with the displacement φ_2 of pendulum 2. The synchronization **90° - 2/1** during which pendulum 2 is delayed to pendulum 1 is also observed. Figure 2(d) shows the basins of attraction of different synchronous configurations, i.e., the initial values β_{10} and β_{20} which lead to particular configuration. As one can see both 90°-1/2 and 90°-2/1 **synchronizations** are dominant. The existence of complete and antiphase synchronizations requires initial values of phase angles β_{10} and β_{20} , for which the difference $\beta_{10}-\beta_{20}$ is close to 0 or 180° (the accurate size of basins of attraction depends on the beam parameters: m_b , k_y and c_y).

The difference between 90°-1/2 and 90°-2/1 synchronizations is explained in Figure 3(a,b). It shows the state of the pendula (velocity versus displacement) at the time when pendulum 1 passes through the lower equilibrium position with positive velocity. During the 90°-1/2 synchronization pendulum 2 reaches the maximum positive displacement as shown in Figure 3(a). When pendulum 2 reaches maximum negative displacement (Figure 3(b)) we observe 90°-2/1 synchronization.

Note, that the difference between complete and antiphase synchronization is manifested by different phase shift of pendulum 2 in respect to pendulum 1 (this phase shift is respectively equal to 90° and 270° for complete and antiphase synchronizations. The difference between 90°-1/2 and 90°-2/1 synchronization can be described in the analogous way, i.e. the phase shift of pendulum 2 in respect to pendulum 1 is equal to 90° for 90°-1/2 synchronization and equal to 270° for 90°-2/1 synchronization (see Figure 3). Let us finally note that due to the fact that the period of the oscillations of the beam is twice smaller than the period of pendula's oscillations (see eqs. (18) and (21)), the change in the phase shift of one of the pendula by 180° does not affect the resultant force with which the pendula act on the beam, and thus does not affect the oscillations of the beam.

4.2. Synchronization of two pendula with different lengths

In the numerical simulations presented in this section we assume that pendulum 1 has length $l_1=1$ and we take the length of pendulum 2 - l_2 as the control parameter. We observe the similar synchronous configurations as in the system with two identical pendula shown in Figure 4(a-d). Figure 4(a) shows the **almost complete synchronization** ($l_2=1.0025$), during which the phase shift between the pendula's displacements is small (not visible in Figure 4(a))

and the amplitudes of the pendula's oscillations are not equal. The phase shift and the differences between the pendula's amplitudes increase with the increase of l_2 . The beam oscillates with the frequency twice larger than the frequency of the pendula. In Figure 4(b) we observe the **almost antiphase synchronization** ($l_2=1.0025$) during which the phase shift between the pendula's displacements is close to 180° , and time series of pendula's oscillations are the same as in the case of almost complete synchronization. The **almost 90° -1/2 (or 90° -2/1) synchronization** ($l_2=1.025$) during which the phase shift of pendula's displacement is close to 90° is described in Figure 4(c). Contrary to the case of identical pendula the main (the second) harmonic of the beam oscillations is not equal to zero. Figure 4(d) presents the basins of attraction of the synchronous configurations (initial values of β_{10} and β_{20} leading to particular synchronous states) for $l_2=1.025$. One can observe that independently of the initial conditions the system tends to the almost 90° -synchronous state. Note that the slight difference in the length of the pendula can drastically change the basins of attraction. Diagram 4(d) presents the basins of attraction for $l_2=1.0250$ while the examples of complete and antiphase synchronizations shown in Figure 4(a) and 4(b) have been calculated for $l_2=1.0025$ (complete and antiphase synchronizations for $l_2>1.005$ do not exist and that is why their basins of attraction are not in Figure 4(d) – see also Figure 5(c)). The structure of the basins of attraction for $l_2<1.005$ is similar to that shown in Figure 2(d). The dominance of the almost 90° -synchronization is explained using the bifurcation diagrams and the energy balances in Figure 5(a-d) and Figure 6(a,b), respectively. Figure 5(a) and 5(c) present the bifurcation diagrams showing the position of pendula 1 and 2 and the beam in the moments when pendulum 1 reaches maximum positive displacement versus the bifurcation parameter l_2 . The diagram of Figure 5(a) starts from $l_2=1.00$ and initial conditions of **90° -synchronization** configuration. Note that for the pendula of the same lengths, when the displacement of pendulum 1 has the maximum the displacement of pendulum 2 is equal to zero which confirms the phase shift of 90° . In this case the beam is at rest and there is no energy transfer between the pendula. The increase of the length of pendulum 2 causes the decrease of the amplitude of pendulum 1 and increases the amplitude of pendulum 2. The phase shift is no longer equal to 90° but close to this value. The increase of the amplitude of the beam oscillations indicates the increase of the energy transmitted from pendulum 1 to pendulum 2 via the beam (compare with Figure 4(c) showing the same type of synchronization for $l_2=1.0250$). The almost **90° synchronization** is observed up to $l_2=1.03$. For larger values of l_2 we observe quasi-periodic oscillations of the system with narrow windows of periodicity (we describe this behavior later - see Figure 7(a-f)). The described changes of pendula's amplitudes and phase shifts are connected with the changes of transmitted energies as can be seen in Figure 5(b). For $l_2=0$ (identical pendula) one has

$$W_1^{SELF} = W_2^{SELF} = W_1^{VDP} = W_2^{VDP},$$

so there is no transfer of energy between the pendula and between the pendula and the beam so the beam is at rest and

$$W_1^{SYN} = W_2^{SYN} = W_{beam} = 0.$$

The energy balances of the pendula are as follows:

$$W_1^{SELF} = W_1^{VDP}$$

$$W_2^{SELF} = W_2^{VDP}$$

The increase in l_2 causes the decrease in the energies W_1^{SELF} (supplied to it) and W_1^{VDP} (dissipated by it) as the result of the decrease in the amplitude of pendulum 1. Additionally, these energies are no longer equal as $W_1^{SELF} > W_1^{VDP}$ so the part of energy W_1^{SELF} is transmitted to the beam as W_1^{SYN} ($W_1^{SYN} > 0$). The energy balance of pendulum 1 is as follows:

$$W_1^{SELF} = W_1^{VDP} + W_1^{SYN}.$$

Part of energy W_1^{SYN} is dissipated by the beam damper and part is transmitted to pendulum 2 as W_2^{SYN} ($W_2^{SYN} < 0$). The energy balance of the beam has the following form:

$$W_1^{SYN} = W_{beam} + |W_2^{SYN}|.$$

The energy balance of pendulum 2, for which energy W_2^{SELF} is smaller than energy W_2^{VDP} is as follows

$$W_2^{SELF} + |W_2^{SYN}| = W_2^{VDP}.$$

The example of energy balance for $l_2=1.025$ is shown in Figure 6(a) (we show the absolute value of negative energy W_2^{SYN}).

The bifurcation diagram of Figure 5(c) starts from $l_2=1.00$ and initial conditions which lead to the **complete synchronization** configuration. One can see that for the case of identical pendula, the pendula's displacements are identical, the displacement of the beam is excited by the resultant force with which the pendula act on the beam and there is no energy transfer between the pendula. The increase of the length of pendulum 2 causes respectively the increase of the amplitude of pendulum 1, the decrease of the amplitude of pendulum 2 and the phase shift close (but not) equal to zero. The change of the beam displacement indicates the change in the phase shifts (compare to Figure 4(a), showing the time series for $l_2=1.0025$). It can be observed that the threshold value of the bifurcation parameter, for which the almost complete synchronization exists is $l_2=1.005$. At this value we observe a bifurcation in which almost complete synchronization loses stability and is replaced by almost 90° synchronous state. Therefore, for $l_2 > 1.005$ the structure of the bifurcation diagram is the same as in Figure 5(a).

The changes in energy values associated with the above described changes of amplitudes and phases are shown in Figure 5(d). As one can see, for $l_2=1.0$ (identical pendula) we have:

$$W_1^{SELF} = W_2^{SELF}$$

$$W_1^{VDP} = W_2^{VDP}$$

$$W_1^{SYN} = W_2^{SYN}.$$

Contrary to the 90° synchronization in the state of complete synchronization (of the system with identical pendula), energy W_1^{SELF} is larger than the absolute value of energy W_1^{VDP} and energy W_2^{SELF} is larger than absolute value of energy W_2^{VDP} so the pendula dissipate only parts of the supplied energies W_1^{SELF} and W_2^{SELF} and the rests of them W_1^{SYN} and W_2^{SYN} are transmitted to the beam and dissipated in the beam damper. The energy balances of the pendula can be expressed as:

$$W_1^{SELF} = W_1^{VDP} + W_1^{SYN}$$

$$W_2^{SELF} = W_2^{VDP} + W_2^{SYN}$$

The energy balance of the beam is as follows:

$$W_{beam} = W_1^{SYN} + W_2^{SYN}.$$

The increase of length l_2 results in the increase of the amplitude of pendulum 1 which increases both energy W_1^{SELF} supplied to the beam and dissipated W_1^{VDP} energy. On the other hand, due to the decrease of the amplitude of pendulum 2, energies W_2^{SELF} and W_2^{VDP} decrease. Contrary to the 90° -synchronization both pendula provide energy to the beam. This energy is entirely dissipated by the beam damper and there is no flow of energy between the pendula. Regardless of whether the lengths of the pendula are the same or different, the system satisfies the above energy balance presented in Figure 6(b) for $l_2=1.0025$.

The bifurcation diagrams which start from 90° -2/1 and antiphase synchronous configurations (for identical pendulums) are not shown as these configurations differ from 90° -1/2 and complete synchronizations only by difference of the phase shift of the pendulum 2 by 180° . As mentioned above, this change in the position of pendulum 2 does not change the resultant force with which the pendula act on the beam and does not change the displacements of the beam. This means that the energy bifurcation diagrams corresponding to these configurations are identical to these shown in Figures 4(b,d).

In the interval $1.0 \leq l_2 < 1.005$ depending on the initial conditions the system can reach one of the four co-existing synchronous states, i.e., almost complete, almost antiphase, almost 90° -1/2 or almost 90° -2/1- synchronization. With further increase of l_2 in the interval $1.005 \leq l_2 \leq 1.03$ one observes only almost 90° -1/2- or almost 90° -2/1-synchronizations. If the system starts in the state of complete- or antiphase-synchronization, when passing through the threshold $l_2=1.005$ the system undergoes bifurcation after which tends to almost 90° -1/2- or almost 90° -2/1- synchronous configurations. In this interval there exist only configurations for which there is the maximum reduction of the forces with which pendula act on the beam.

The behavior of the system for $l_2 > 1.03$ is explained in Figure 7(a-f). Figure 7(a) shows the almost 90° -1/2-synchronous configuration (note the similarity to Figure 3(a) showing the configuration of identical pendula). One can see that for $l_2 > 1.0$, the phase shift is close but smaller than 90° , both pendula oscillate with the same frequency. The increase of the value of l_2 causes that the pendula are not synchronized and their oscillations are quasi-periodic as shown in Figure 7(b) ($l_2=1.035$). In Figure 7(c) we present the bifurcation diagram for $1.3 < l_2 < 1.4$. Notice the periodic windows in the neighborhoods of the rational values of l_2

(arrows indicate windows for $l_2 = 1.31 \approx 1.306 = \frac{64}{49} = \left(\frac{8}{7}\right)^2$ and

$l_2 = 1.3659 \approx 1.361 = \frac{49}{36} = \left(\frac{7}{6}\right)^2$). For these values of l_2 the oscillations of the system are

periodic (in the period of r oscillations of pendulum 1, pendulum 2 oscillates s times). The periodic windows do not occur exactly at the rational values of l_2 but close to them because the oscillations of the beam change the periods of the pendula (in comparison to the period of the pendula mounted to the nonmovable beam). Figure 7(d) presents the enlargement of Figure 7(c) for $1.365 < l_2 < 1.366$. For $l_2=1.3659$ the system oscillates with period 7 as can be seen in Figure 7(e). The width of the periodic window in the neighborhood of $l_2=1.3659$ is so small that the slight change of l_2 (e.g. $l_2=1.3658$) causes that the oscillations are quasiperiodic as shown in Figure 7(f).

4.3 Synchronization of three identical pendula

Figure 8(a-d) shows synchronous configurations predicted in Sec. 3. In Figure 8(a) one observes the **complete-synchronization**, during which all pendula oscillate in the same way ($\varphi_1 = \varphi_2 = \varphi_3$) and the beam oscillates with the frequency twice larger than the frequency of the pendula. The **antiphase-2-1-synchronization**, during which the displacement of one of the pendula (e.g. φ_3) is the mirror image of the displacements of the cluster of two other pendula ($\varphi_1 = \varphi_2$) is shown in Figure 8(b). The beam oscillates with the frequency twice larger than the frequency of the pendula as in complete synchronization. Figure 8(c) presents **120° -1/2/3-synchronization** during which the phase differences between pendula are equal to 120° and main (the second) harmonic of the beam oscillations is equal to zero so the beam is nearly at rest. In Figure 8(d) we show **60° -1/3/2-synchronization**, during which the phase shift between the pendula's displacements is equal to 60° and main (the second) harmonic of the beam oscillations is equal to zero so the beam is nearly at rest.

Two types of 120° -synchronization are shown in Figure 9(a-b). Figure 9(a) presents 120° -1/2/3-synchronization during which the displacement φ_1 of pendulum 1 is phase delayed by 120° in comparison to displacement φ_2 of pendulum 2, and displacement φ_2 is delayed in comparison to displacement φ_3 of pendulum 3 also by 120° . In Figure 9(b) we present 120° -1/3/2-synchronization in which the displacement φ_1 is phase delayed in comparison to displacement φ_3 by 120° and displacement φ_3 is delayed in comparison to displacement φ_2 by 120° . In the system with three identical pendula, of course, there is no difference between these two configurations, in addition to different numbers of pendula. Significant differences between them appear in the next section, when we diversify the length of the pendula. Figure 9(c-e) shows, how the change of the position of one pendulum leads to the change of 120° -1/2/3 synchronous configuration into one of three types of 60° -synchronization. In Figure 9(c) the change of the position of pendulum 3 leads to 60° -1/3/2-synchronization, during which displacement φ_3 of pendulum 3 is phase shifted ahead by 60° in relation to the displacement φ_1 of pendulum 1 and phase delayed by 60° to displacement φ_2 of pendulum 2. Figure 9(d) describes the case when the change of the position of pendulum 2 causes transition to 60° -3/2/1-synchronization, during which displacement φ_2 of pendulum 2 is phase ahead of the displacement φ_3 of pendulum 3 by 60° and is delayed to the displacement φ_1 of pendulum 1 by 60° . In Figure 9(e) the change of the position of pendulum 1 leads to 60° -2/1/3-synchronization during which the displacement φ_1 of pendulum 1 is ahead of the displacement φ_2 of pendulum 2 and delayed to the displacement φ_3 of pendulum 3 by 60° . Figure 9(f-h) shows the analogous transitions of 120° -1/2/3-synchronous configuration into one of three 60° -synchronization configurations.

As in the system with two pendula the change of the position of any pendula by 180° does not affect the change of the resultant force with which the pendula act on the beam. There are two distinct energy balances on the system. The first one is characteristic for the 120° -1/2/3-synchronization (Figure 9(a)) and all 60° -synchronization configurations obtained by the change of the position of one of the pendula (pendulum 3 in Figure 9(c), pendulum 2 in Figure 9(d) and pendulum 1 in Figure 9(e)) and the second one is characteristic for 120° -1/3/2-synchronization configuration (Figure 9(b)) and all configurations of Figure 9(f-h).

4.4. Synchronization of three pendula with different lengths

In numerical simulations presented in this section we assume that pendulum 1 has the dimensionless length $l_1=1$, pendulum 2 $l_2 = 0.5(l_1+l_3)$ and take the length of pendulum 3 l_3 as a control parameter (we consider that the length of pendulum 2 is the mean value of the lengths of other pendula).

Our simulations show that there is the transfer of energy between the pendula which causes that the pendula oscillate with different amplitudes. We identify six different synchronous configurations shown in Figure 10(a-f) which are analogous to the configurations of the system with identical pendula. Figure 10(a) presents the *almost complete synchronization* ($l_3=1.005$), during which there is a small phase shift (not visible in Figure 10(a)) of the pendula's displacements and the pendula's amplitudes are not equal. The differences in the phase shifts and amplitudes increase with the increase of l_2 and l_3 . The beam oscillates with the frequency twice larger than the frequency of the pendula. The *almost antiphase 2/1-synchronization* ($l_3=1.005$) is shown in Figure 10(b). Two pendula (1 and 3) are in the state of the almost complete synchronization (for identical pendula there is a cluster of two identically oscillating pendula). The phase shift between these pendula and pendulum 2 is close to 180° . The amplitudes of pendula are the same as in the case of the almost complete synchronization (Figure 10(a)). Both configurations differ only by the phase shift of pendulum 2 equal to 180° . Figure 10(c) presents *almost 120° -1/2/3 synchronization*

($l_2=1.005$) during which the phase shifts between pendula's displacements are close to 120° . Contrary to the case of identical pendula the main (the second) harmonic of the beam oscillations is not equal to zero and we observe the transfer of energy between the pendula. In Figure 10(d) we show **almost 60° -1/3/2 synchronization** ($l_2=1.005$) during which the displacement φ_3 of pendulum 3 is ahead of the displacement φ_1 of pendulum 1 and is phase delayed to the displacement φ_2 of pendulum 2 by 60° . As this configuration differs from the configuration of **almost 120° -1/2/3-synchronization** (shown in Figure 10(c)) only by the phase shift of pendulum 3 (the difference close to 180°) pendula's and beam's displacements in Figure 11(c) and Figure 11(d) are the same. Figure 10(e) shows **almost 120° -1/3/2-synchronization** ($l_2=1.005$) during which the phase shifts between pendula's displacements are close to 120° . Note that the pendula's amplitudes are different than these shown in Figure 11(c) as there is different energy balance in both cases and the distinction between almost 120° -1/2/3 and almost 120° -1/3/2 synchronizations is justified (beside the fact that for identical pendula these configurations are equivalent). The **almost 60° -1/2/3 synchronization** ($l_2=1.005$) during which the displacement φ_2 of pendulum 2 is ahead of displacement φ_1 of pendulum 1 and phase delayed to displacement φ_3 of pendulum 3 by 60° is described in Figure 10(f). As this configuration differs from **120° -1/3/2 synchronization** only by the phase of pendulum 2, the displacements of the beam and pendula in Figure 10(e) and 10(f) are the same.

Figure 11(a,b) shows the basins of attraction of various synchronous configurations, i.e., the domains of initial conditions β_{20} and β_{30} leading to particular configuration (we assume $\beta_{10}=0^\circ$). Figure 11(a) has been calculated for the case of identical pendula ($l_1=l_2=l_3=1.0$), and Figure 11(b) for the pendula with different lengths: $l_1=1.0$, $l_2=1.0025$, $l_3=1.005$. Note that slight differences in the pendula's lengths cause the disappearance of the basins of almost complete and almost antiphase synchronizations. Independently of the initial conditions the system tends to the synchronous configurations during which the beam is nearly at rest, i.e., almost 60° - and almost 120° - synchronizations.

The analysis of synchronous configuration in the system with three pendula of different lengths predicts the existence of three different energy balances and three qualitatively different types of bifurcation diagrams which show the dependence of oscillations' amplitudes, phase angles and the energies transferred between the pendula.

The examples of bifurcation diagrams and energy balances are shown respectively in Figure 12(a-f) and Figure 13(a-c). Figure 12(a,c,e) presents the positions of pendula 1-3 and the beam at the time when the displacement of pendulum 1 reaches the maximum positive value. The changes in the pendula's positions are associated with the changes of the appropriate energies as can be seen in the energy bifurcation diagrams of Figure 12(b,d,f).

In the simulations described in Figure 12(a,b) we start with $l_3=1.00$ and initial conditions leading to the configuration of **120° -1/2/3 synchronization**. Note that for the pendula with the same length when the displacement of pendulum 1 reaches maximum, the displacements of pendula 2 and 3 are equal and smaller (Figure 8(c) and Figure 9(a) shows the details of this configuration). The beam is at rest so there is no energy transfer between the pendula. For $l_3=1.0$ one has

$$W_1^{SELF} = W_2^{SELF} = W_3^{SELF} = W_1^{VDP} = W_2^{VDP} = W_3^{VDP},$$

each pendulum dissipates the whole energy which is supplied to it so the beam is at rest, i.e.,

$$W_1^{SYN} = W_2^{SYN} = W_3^{SYN} = W_{beam} = 0.$$

The energy balance of the pendula is as follows:

$$W_1^{SELF} = W_1^{VDP}$$

$$W_2^{SELF} = W_2^{VDP}$$

$$W_3^{SELF} = W_3^{VDP}$$

The increase of the lengths of pendula 2 and 3 causes that the amplitudes of the pendula's oscillations become different. The decrease of the values of W_1^{SELF} and W_3^{SELF} show that the amplitudes of pendula 1 and 3 decrease. The increase of W_2^{SELF} show that the amplitude of pendulum 2 increases. The part of the energy supplied to pendula 1 and 3 (W_1^{SELF} and W_3^{SELF}) is transmitted to the beam as W_1^{SYN} and W_3^{SYN} . The energy balance of the pendula is as follows

$$W_1^{SELF} = W_1^{VDP} + W_1^{SYN}$$

$$W_3^{SELF} = W_3^{VDP} + W_3^{SYN}.$$

Small part of energy $W_1^{SYN} + W_3^{SYN}$ is dissipated in the beam damper so one has the following energy balance of the beam:

$$W_1^{SYN} + W_3^{SYN} = W_{beam} + |W_2^{SYN}|.$$

The rest of energy $W_1^{SYN} + W_3^{SYN}$ is obtained by pendulum 2 as W_2^{SYN} (negative) in the case when W_2^{SELF} is smaller than W_2^{VDP} . One has the following energy balance of pendulum 2:

$$W_2^{SELF} + |W_2^{SYN}| = W_2^{VDP}.$$

The above energy balances are shown in Figure 13(a) for $l_3=1.0051$ (the energy W_{beam} is small so it is not visible). On the left hand side of the diagram, the energy supplied to the system, i.e., $W_1^{SELF} + W_2^{SELF} + W_3^{SELF}$ is shown. The energy dissipated in the system: $W_1^{VDP} + W_2^{VDP} + W_3^{VDP} + W_{BEAM}$ is indicated on the right hand side. The energy streams flow from left to right, e.g. diagonal slanted line in Figure 13(a) indicates the energy stream W_1^{SYN} (going from pendulum 1 to pendulum 2) which together with the energy W_3^{SYN} is equal to the energy dissipated by pendulum 2 i.e., W_2^{SYN} .

Figure 12(a,b) shows that the threshold value of the bifurcation parameter for which we observe **almost 120°-1/2/3 synchronization** is $l_3=1.0075$. For larger values of l_3 one observes only quasi-periodic oscillations (see Figure 14).

In the simulation shown in Figure 12(c,d) we start at $l_3=1.00$ and initial conditions leading to **120°-1/3/2 synchronization** (for identical pendula this configuration is equivalent to **120°-1/2/3 synchronization** and the energy balances are identical).

The increase of the lengths of pendula 2 and 3 causes that the amplitudes of pendula's oscillations become different. Energies W_2^{SELF} and W_3^{SELF} are not equal and energy W_1^{SELF} increases. In this configuration pendula 2 and 3 transmit energy to the beam and through it to pendulum 1 so:

$$W_2^{SELF} = W_2^{VDP} + W_2^{SYN}$$

$$W_3^{SELF} = W_3^{VDP} + W_3^{SYN}.$$

$$W_1^{SELF} + |W_1^{SYN}| = W_1^{VDP}.$$

Small part of energy $W_2^{SYN} + W_3^{SYN}$ is dissipated by the beam damper and the energy balance of the beam is as follows:

$$W_2^{SYN} + W_3^{SYN} = W_{beam} + |W_1^{SYN}|.$$

The above energy balances are shown in Figure 13(b) for $l_3=1.0051$ (the energy W_{beam} is small so it is not visible).

For $l_3=1.0058$ almost 120°-1/3/2-synchronization loses stability and the system reaches the energy state of almost 120°-1/2/3 synchronization configuration (see Figure 12(d)). Note that in the interval $1.058 < l_3 < 1.078$ Figure 12(d) and Figure 12(b) are identical. In Figure 12(c)

one can see that the system has almost 60° -2/1/3 synchronization configuration shown in Figure 9(c). Note that for different state of the system (different displacements and velocities of the pendula and the beam) in the moment of the change of bifurcation parameter the system can reach almost 60° -1/3/2 or 60° -3/2/1 configurations. Figure 12(e,f) shows the bifurcation diagrams which start at $l_3=1.00$ and initial conditions which lead to the **complete synchronization**. As can be seen in the case of identical pendula the displacements of all pendula are identical and the beam oscillations are excited by the resultant force with which pendula act on it. There is no energy transfer between the pendula, energies W_i^{SELF} are larger than energies W_i^{VDP} so all pendula transfer energy W_i^{SYN} to the beam (dissipated in the beam damper):

$$W_1^{SELF} = W_1^{VDP} + W_1^{SYN}$$

$$W_2^{SELF} = W_2^{VDP} + W_2^{SYN}$$

$$W_3^{SELF} = W_3^{VDP} + W_3^{SYN}$$

Energy balance of the beam is as follows:

$$W_{beam} = W_1^{SYN} + W_2^{SYN} + W_3^{SYN}.$$

The increase of l_2 causes the changes of the oscillations' amplitudes and the values of all energies. However, in the interval $1.0 < l_3 < 1.0039$ the above energy balances are fulfilled. For larger values of l_3 ($l_3 > 1.0039$) the energy W_1^{SYN} becomes negative and pendulum 1 starts to gain energy from pendula 2 and 3. Numerical examples of the energy balances are shown in Figure 13(c) for $l_3=1.0051$. At $l_3=1.0054$ the almost complete-synchronization configuration loses its stability and the system bifurcates to almost 60° -3/1/2 synchronization configuration (Figure 12(f)). The energy balance of this configuration is the same as one of almost 120° -1/3/2 synchronization configuration. At $l_3=1.0058$ (see Figure 12(e,f)) almost 60° -3/1/2 synchronization configuration loses its stability and the system bifurcates to the almost 120° -1/2/3-synchronization configuration. Note that in the interval $1.0054 < l_3 < 1.0058$ Figure 12(f) and Figure 12(d) are identical and in the interval $1.0058 < l_3 < 1.0078$ Figure 12(f) and Figure 12(b) are identical.

To summarize in the interval $1.0 < l_3 < 1.0054$ all synchronous configurations (almost complete, almost antiphase, almost 120° and almost 60° –synchronizations) coexist, i.e., we have 12 possible synchronous configurations during which the system is characterized by three distinct energy balances. For $1.0054 < l_3 < 1.058$ almost 120° - and almost 60° -synchronizations coexist, i.e., we have 8 configurations with two different energy balances (of 120° -1/2/3 and 120° -1/3/2 synchronizations). In the interval $1.0058 < l_3 < 1.078$ one observes 4 synchronous configurations characterized by the same energy balance (of 120° -1/2/3-synchronization). As in the case of the system with two pendula there exists l_3 -interval ($1.0054 < l_3 < 1.0078$) in which one observes only such synchronous configurations in which the forces transmitted by pendula to the beam reduce each other (the resultant force is small).

Finally, let us consider Figure 14(a-e) describing the behavior of the system for $l_3 > 1.0078$. Figure 14(a) shows 120° -1/2/3 synchronization configuration for $l_3=1.005$ (note the similarities to the schematic description of this configuration in the case of identical pendula shown in Figure 9(a)). Single points in Figure 14(a) indicate period one oscillations. The angles 120° and 240° allow observing how close to these values the observed phase shifts between the pendula are. In Figure 14(b) we show energetically equivalent configuration of the 60° -1/3/2 synchronization for the same values of $l_3=1.005$. The angles 60° 120° allow to observe how close to these values the phase shifts between the pendula are. The comparison of Figure 14(a) and 14(b) confirms that shown configurations differ only by the change of the position of pendulum 3 by 180° . Figure 14(c) shows the configuration of the almost complete-synchronization for $l_3=1.005$. In Figure 14(d) we show the positions of pendula for $l_3=1.008$ (larger than critical value 1.0078). The replacement of the single points by the closed curves

indicates quasi-periodic oscillations. Figure 14(e) presents the bifurcation diagram of the system in the following range of control parameter $1.3 < l_3 < 1.4$. Contrary to the case of two pendula (Figure 7(c)) one cannot observe the periodic windows and for $l_3 = 1.078$ we have observed only quasiperiodic oscillations.

4.5. Synchronization of the systems with larger number of pendula

To explain the behavior of the system with larger number of pendula let us consider Figure 15(a-d) and Figure 16(a-c). Figure 15(a) presents the bifurcations diagram (analogous to that of Figure 5(c) and 12(e)). The length of pendulum 5 l_5 ($1 \geq l_5 \geq 1.008$) has been taken as a bifurcation parameter. The length of pendulum 1 is equal to 1 and the lengths of the rest of the pendula are changing according to the following relations:

$$l_2 = 0.25(l_1 + l_5)$$

$$l_3 = 0.50(l_1 + l_5)$$

$$l_4 = 0.75(l_1 + l_5)$$

The diagram starts from the state of complete synchronization for $l_5 = 1.0$ (identical pendula). In the interval $1.0 < l_5 < 1.055$ we observe an almost complete synchronization. Different lengths of the pendula cause that the pendula's amplitudes are different as can be seen in Figure 15(b) for $l_5 = 1.004$. Poincare map shown in Figure 15(c) allows the observation of the phase shifts between the pendula. These shifts are small (close to zero) that justifies the term almost complete synchronization. The passage through the threshold value $l_5 = 1.0055$ causes that the oscillations of the pendula become quasi-periodic as can be seen on Poincare map in Figure 15(d) ($l_5 = 1.006$). Note that 5 single points in Figure 15(c) have been replaced by 5 closed curves.

The complete synchronization as described in Figure 15(a-d) occurs (for the open set of the appropriately selected initial conditions) in the systems of n pendula (we performed our calculations up to 100 pendula). This synchronization co-exists with almost anti phase synchronization of two clusters with r and $n-r$ synchronized pendula ($r = 1, \dots, n-1$). The almost complete-synchronization and almost antiphase-synchronization can co-exist as they are energetically identical. (The only difference is the change of the phase of one or several pendula by 180° which does not change the energy balance of the system).

Almost complete- and almost antiphase-synchronizations belong to the first kind of synchronizations during which the forces with which the pendula act on the beam are added and the oscillations of the pendula are accompanied by large oscillations of the beam. The frequency of the beam's oscillations is twice larger than the frequency of the pendula.

In the systems with $n \geq 4$ we have not observed the synchronizations of the second kind during which the forces with which the pendula act on the beam partially reduce each other. Theoretical justification of this statement is as follows: the phase shifts between the pendula in the state of phase synchronization have to satisfy the conditions, which in the case of the system of identical pendula, are given by eqs. (23). These equations have explicit solutions β_2 and β_3 for the systems with three pendula - see eq. (25) but for larger number of pendula eqs. (23) constitute a system of two equations with three or more unknowns and have infinitely many solutions. For the systems with identical pendula, this means that in the steady state the motion of the system is periodic but the phase shifts between pendula are not constant and independent of the initial conditions (within the basin of attraction configuration). The phase shift which is dependent on the initial conditions cannot characterize the synchronization configuration. Although the phase shifts are constant their values depend on the initial conditions and are subject to change after any external perturbations of the pendula's or beam oscillations. These do not fulfill the definition of synchronization. In the systems of pendula with different lengths (generally, with pendula, which mounted to the nonmovable beam have

different periods of oscillations) practically only quasiperiodic oscillations can be observed. Figure 16(a) shows the bifurcation diagram which starts at $l_5=1.0$ and different initial conditions from that considered in Figure 15(a). The oscillations of the system for $l_5=1.0$ are periodic as can be seen on Poincare map shown in Figure 16(b). Note that the differences between the phases of neighboring pendula are identical and equal to 72° . After the perturbation the oscillations are periodic again but the differences between the phases of the pendula are different than before the perturbation as can be seen in Figure 16(c) (the phase shifts between the pendula are constant, but their constant values are neither characteristic nor independent on initial conditions). Arbitrarily small increase in l_5 leads to quasi-periodic oscillations as is evident in Figure 16(a) ($l_5=1.0012$).

To sum up, in systems with multiple pendulums, there is no phase synchronization and the sufficiently large differences in the lengths of pendula cause that the complete and antiphase synchronization, during which the oscillations of the beam are large, are not observed. Generally, we have not observed the synchronous states in which the resultant force with which the pendula act on the beam is large.

5. Conclusions

In the system consisting of a number of van der Pol's pendula mounted on the rigid beam which can oscillate in the vertical direction we observe the phenomenon of synchronization of two and three nonidentical (with different lengths) pendula. During the synchronous motion the oscillations of the pendula are periodic and the phase shifts between the pendula displacements (nearly harmonic) are constant and characterize the particular pendula's configurations. The values of the phase shifts do not depend on initial conditions (within the basin of attraction of the particular configuration). Several synchronized configurations can coexist for the same system's parameters.

We identify two kinds of synchronous configurations. Configurations of the first kind are characterized by the large resultant force with which pendula act on the beam. This force excites the beam oscillations with large amplitude and frequency twice larger than the frequency of the pendula. These configurations are: (i) almost complete synchronization during which all pendula oscillate in the same way, (ii) almost antiphase synchronization of two clusters of completely synchronized pendula (the numbers of pendula in both clusters depend on initial conditions). Energy balance of the system in both configurations is the same, differing only in the phase change of one or more pendula by 180° . This difference does not affect the oscillations of the beam. Synchronization of the first kind can occur in systems with arbitrarily large number of pendula, provided that the differences between the lengths of the pendula are sufficiently small. The configurations of the second kind are characterized by the small value of the resultant force with which pendula act on the beam. As the result the beam oscillates with small amplitude. These configurations are: (i) almost 90° -synchronization of two pendula shifted in phase, (ii) almost 60° or 120° -synchronizations of three pendula. Synchronization of the second kind does not occur in systems with more than three pendula. In such systems besides the first type of synchronization we observe quasi-periodic oscillations.

The synchronous motion of pendula can occur because the pendula can transfer part of the energy supplied to them between themselves. In the case of identical pendula the energy flow vanishes after reaching the state of synchronization. In the case of pendula with different lengths, the flow of energy occurs even after reaching the synchronous state as the pendula oscillate with the same frequency but with different amplitudes. The energy flow is possible as the result of beam oscillations. In the system with pendula of different lengths, in all synchronized configurations we observe that the amplitude of oscillations of some pendula increases while the amplitude of the rest of pendula decreases. During oscillations one group

of pendula (with decreased amplitude) drive the beam (causing its oscillations, and in turn the oscillations of the beam increase the amplitudes of other pendula. Therefore, there is a constant flow of energy via the beam. Since the changes of the amplitudes of pendula's oscillations caused by the beam's oscillations, lead to the changes in pendula's periods, it is possible to obtain the steady state in which the periods of oscillations of all pendula reach the common value in the state of synchronization.

In the system of identical pendula we found the synchronous configurations in which the beam is practically stationary (the amplitude of the fundamental, second harmonic of beam oscillations is equal to zero). In the system with different pendula, in which pendula transmit the energy between themselves, the beam oscillates during each synchronous configuration as the oscillations of the beam are the main factor in the energy transfer mechanism.

In systems with identical pendula at the state of complete or antiphase synchronization the resultant force with which the pendula act on the beam is large and excites the oscillations of the beam with large amplitude. In many practical systems large amplitudes of the beam can be undesired. The results of the presented studies show how to avoid the risk of complete-synchronization by varying the lengths of the pendula. In this case the complete (or antiphase)-synchronization becomes unstable and the system independently of the initial conditions reaches the state of almost 90° (60° or 120°) – synchronization or shows quasi-periodic behavior which eliminates the risk of large amplitudes of the beam's oscillations.

Contrary to the case of the pendula with the escapement mechanism (clocks) [26,27] in the considered system we have not observed chaotic behavior.

Acknowledgment: This work has been supported by the Foundation for Polish Science, Team Program – Project No. TEAM/2010/5/5.

References

1. A. Pikovsky, M. Resenblum, and J. Kurths, *Synchronization: An Universal Concept in Nonlinear Sciences*, (Cambridge University Press, Cambridge, 2001).
2. I.I. Blekham, *Synchronization in Science and Technology*, (ASME, New York, 1988).
3. S. H. Strogatz, I. Stewart, *Scient. Am.*, 269 (1993) 102-109.
4. S. H. Strogatz, *Sync: The Emerging Science of Spontaneous Order*, (Penguin Science, London, 2004).
5. E. Rodriguez, N. George, J.-P. Lachaux, J. Martinerie, B. Renault, F.J. Varela, *Nature* 397 (1999) 430-433.
6. M. M. Abdulrehem, E. Ott, *Chaos* 19 (2009) 013129.
7. S. Boccaletti, Louis M. Pecora and A. Pelaez, *Phys. Rev. E* 63 (2001) 066219.
8. P. Dallard, A. J. Fitzpatrick, A. Flint, S. Le Bourva, A. Low, R. M. R. Smith, M. Willford, *Struct. Eng.* 79 (2001) 17-33.
9. P. Dallard, A. J. Fitzpatrick, A. Flint, A. Low, R. M. R. Smith, M. Willford, M. Roche, *J. Bridge Eng.* 6 (2001) 412-417.
10. B. Eckhardt, E. Ott, S. H. Strogatz, D. Abrams, A. McRobie, *Phys. Rev. E* 75 (2007) 021110.
11. S. Nakamura, *J. Struct. Eng.* 130 (2004). 32-37.
12. S. H. Strogatz, D. M. Abrams, A. McRobie, B. Eckhardt, and E. Ott, *Nature*, 438 (2005) 43-44.
13. S. Boccaletti, J. Kurths, G. Osipov, D.L. Valladares and C. Zhou, *Phys. Rep.* 366 (2002) 1-101.

14. S. Boccaletti, V. Latora, Y. Moreno, M. Chavez, D.-U. Hwang, Phys. Rep., 424, (2006) 175–308.
15. C. Huygens, *Horologium Oscilatorium*, (Apud F. Muquet, Parisiis, 1673); English translation: *The pendulum clock*, (Iowa State University Press, Ames, 1986).
16. C. Huygens, Letter to de Sluse, In: *Oeuvres Complètes de Christian Huygens* (letters; no. 1333 of 24 February 1665, no. 1335 of 26 February 1665, no. 1345 of 6 March 1665), (Société Hollandaise Des Sciences, Martinus Nijhoff, La Haye, 1893)
17. B. van der Pol, and J. van der Mark, J., *Nature*, **120**, 363-364, (1927)
18. A. Yu. Pogromsky, V.N. Belykh, and H. Nijmeijer, Controlled synchronization of pendula, in Proceedings of the 42nd IEEE Conference on Design and Control (2003), Maui, Hawaii, pp. 4381-4385.
19. M. Bennet, M. F. Schatz, H. Rockwood, and K. Wiesenfeld, Proc. Roy. Soc. London, A **458**, 563-579 (2002).
20. M. Senator, J. Sound and Vibration, **291**, 566-603, (2006).
21. R. Dilao, Chaos, **19**, 023118 (2009).
22. M. Kumon, R. Washizaki, J. Sato, R.K.I. Mizumoto, and Z. Iwai, Controlled synchronization of two 1-DOF coupled oscillators, in Proceedings of the 15th IFAC World Congress, Barcelona, 2002.
23. A.L. Fradkov, and B. Andrievsky, Int. J. Non-linear Mech., **42**, 895 (2007).
24. J. Pantaleone, Am. J. Phys., **70**, 992 (2002).
25. H. Ulrichs, A. Mann, and U. Parlitz, Chaos **19**, 043120, (2009).
26. K. Czolczynski, P. Perlikowski, A. Stefanski, T. Kapitaniak, Prog. Theor. Phys., **122**, (2009) 1027-1033.
27. K. Czolczynski, P. Perlikowski, A. Stefanski, T. Kapitaniak, Physica A, **388** (2009) 5013-5023.
28. K. Czolczynski, P. Perlikowski, A. Stefanski, T. Kapitaniak, Int. J. Bifur. Chaos, **21**, (2011) 2047-2056.
29. K. Czolczynski, P. Perlikowski, A. Stefanski, T. Kapitaniak, Chaos, **21** (2011) 023129
30. K. Czolczynski, P. Perlikowski, A. Stefanski, T. Kapitaniak, Prog. of Theor. Phys., **125** (2011) 1-18.
31. G.L. Baker, J. A. Blackburn and H.J.T. Smith, Phys. Rev. Lett., **81** (1998) 555-559.
32. A. Teufel, A. Steindl and H. Troger, Communications in Nonlinear Science and Numerical Simulation, **11** (2006) 577–594.
33. A. Gavrielides, T. Kottos, V. Kovanis, and G. P. Tsironis, Phys. Rev. E **58** (1998) 5529–5534.
34. Sunghwan Rim, Myung-Woon Kim, Dong-Uk Hwang, Young-Jai Park, and Chil-Min Kim, Phys. Rev. E **64** (2001) 060101.
35. U. E. Vincent, J. A. Laoye, and A. Tella, Int. J. of Modern Physics B, **24**, (2010) 3311-3321
36. J. Peña-Ramírez, R.H.B. Fey, H. Nijmeijer, Nonlinear Theory and Its Applications, IEICE, **12** (2012) 128-142.
37. S. F. Brandt, B. K. Dellen, and R. Wessel, Phys. Rev. Lett. **96** (2006) 034104
38. R. Chacón, P.J. Martínez, J.A. Martínez, S. Lenci, Chaos, Solitons & Fractals,, (2009) 2342–2350

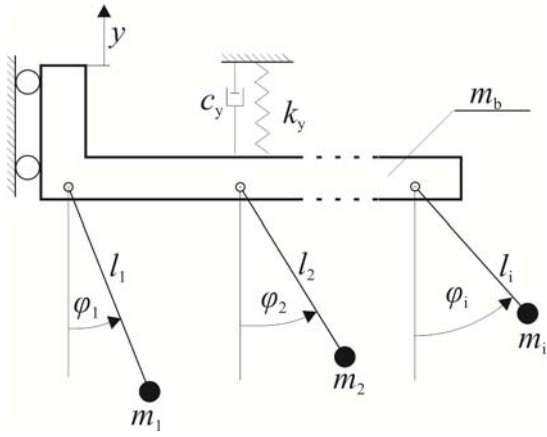


Figure 1. The model of the system.

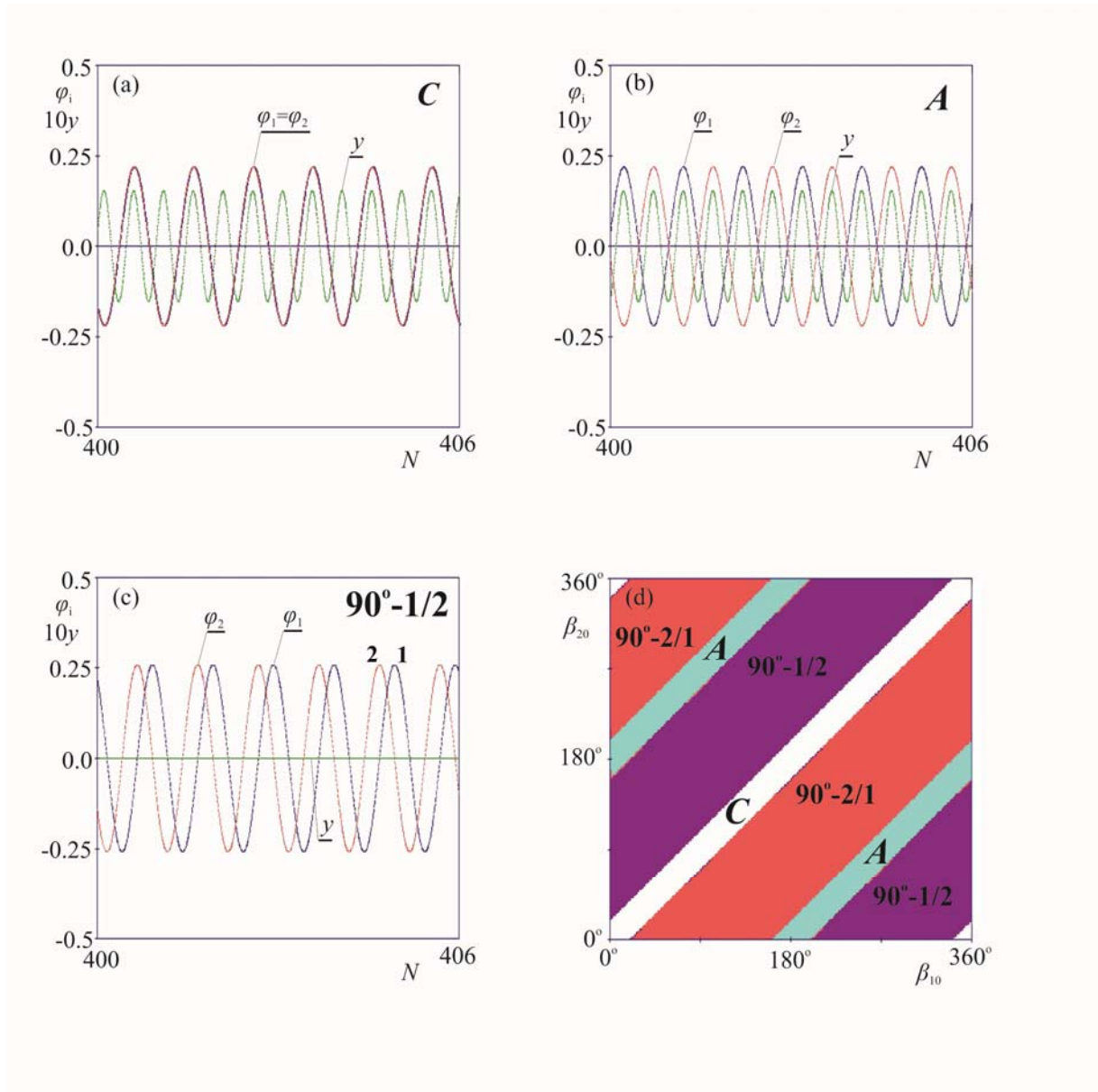
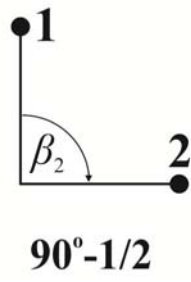


Figure 2. Synchronous configurations in system (3,4) with two identical pendula; (a) time series of complete-synchronization (C), (b) time series of antiphase-synchronization (A), (c) time series of 90° -synchronization, (d) basin of attraction of different types of synchronization.

(a)



(b)

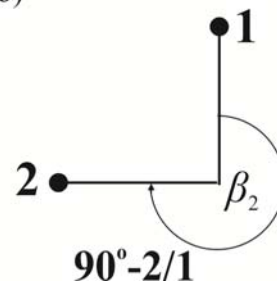


Figure 3. Scheme of 90° -synchronization on the phase plane; (a) $90^\circ-1/2$ -synchronization; (b) $90^\circ-2/1$ -synchronization.

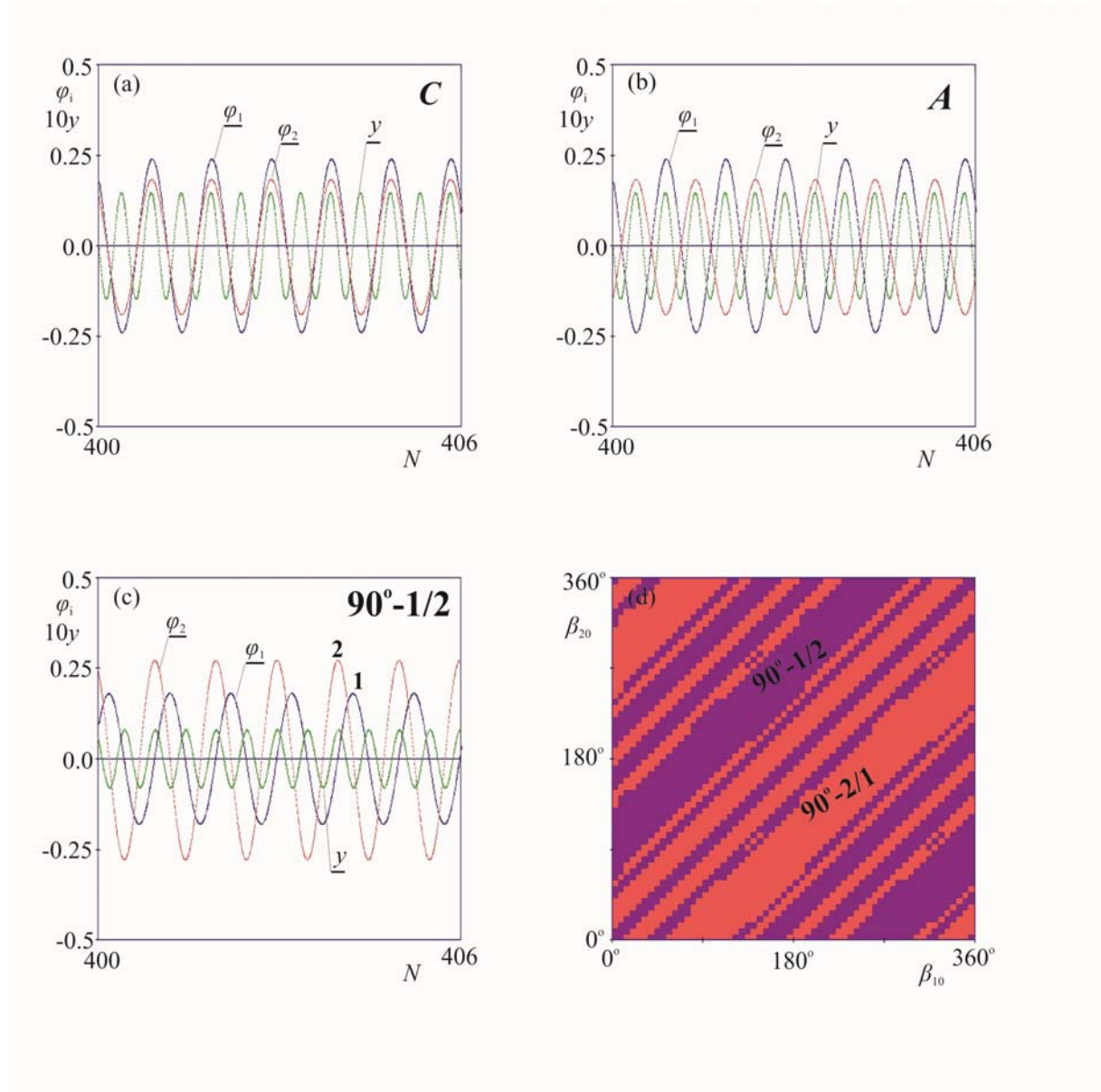


Figure 4. Synchronous configurations in system (3,4) with two nonidentical pendula; (a) time series of almost complete-synchronization (C), $l_2=1.0025$; (b) time series of almost antiphase-synchronization (A), $l_2=1.0025$; (c) time series of almost 90° - synchronization, $l_2=1.025$; (d) basins of attraction of almost 90° - $1/2$ and 90° - $2/1$ configurations, $l_2=1.025$.

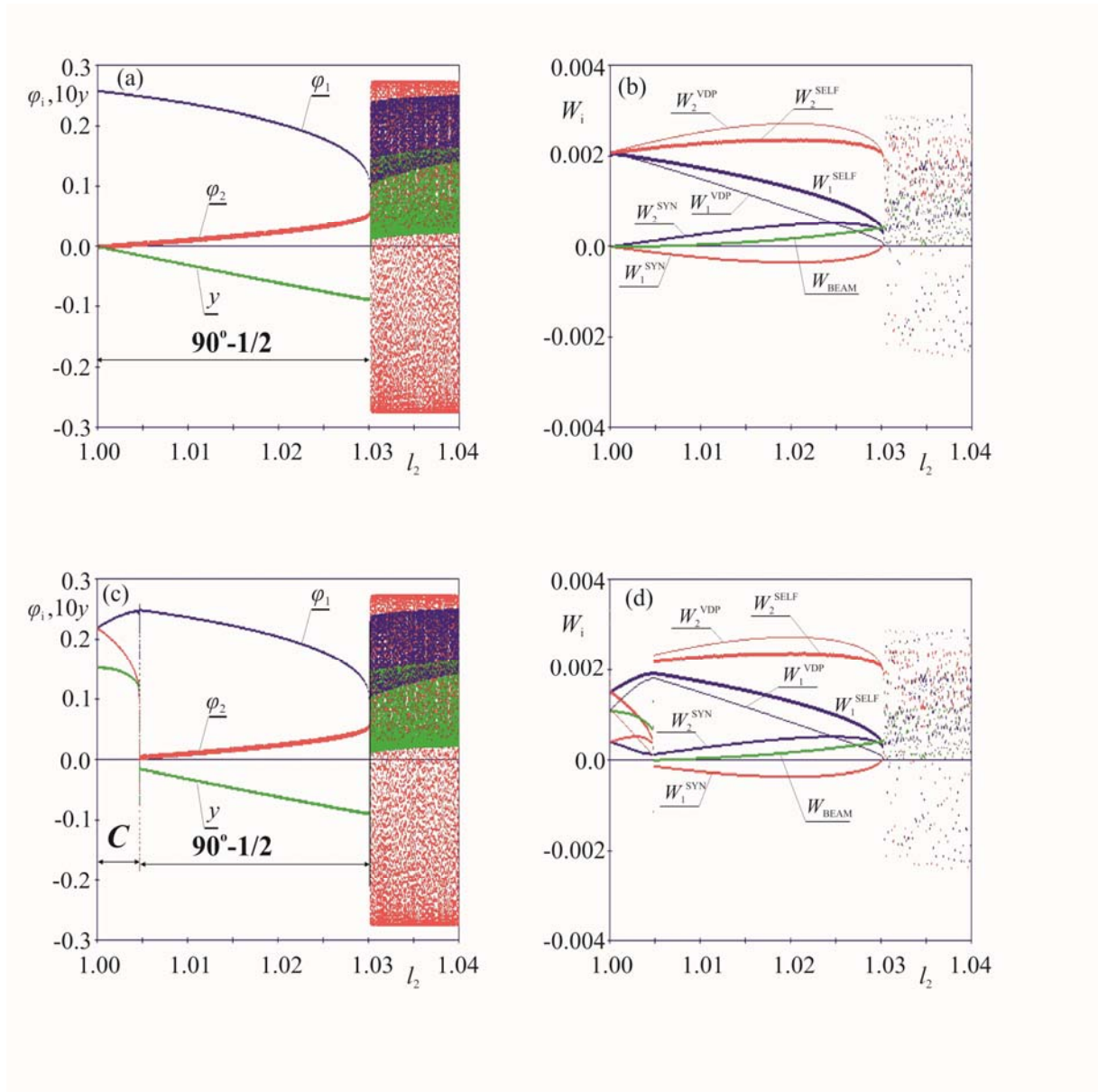


Figure 5. Bifurcation diagrams of system (3,4) with two pendula; (a) from 90° -synchronization to quasi-periodic motion - displacements; (b) from 90° -synchronization to quasi-periodic motion - energies; (c) from complete-synchronization (C) through almost 90° -synchronization to quasi-periodic motion - displacements; (d) from complete-synchronization through almost 90° -synchronization to quasi-periodic motion - energies;

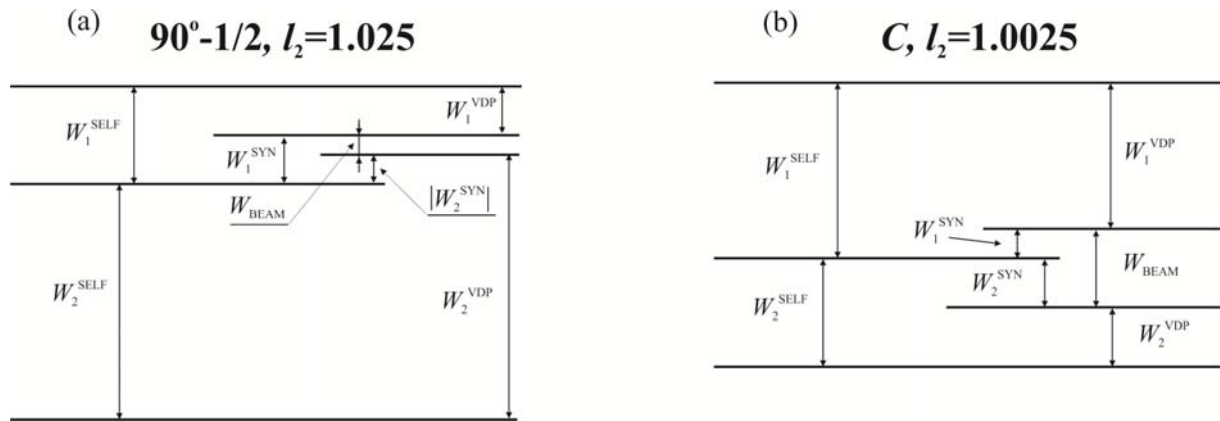


Figure 6. Energy balances of system (3,4) with two pendula; (a) almost 90°-1/2-synchronization for $l_2=1.025$; (b) almost complete-synchronization (C) for $l_2=1.0025$.

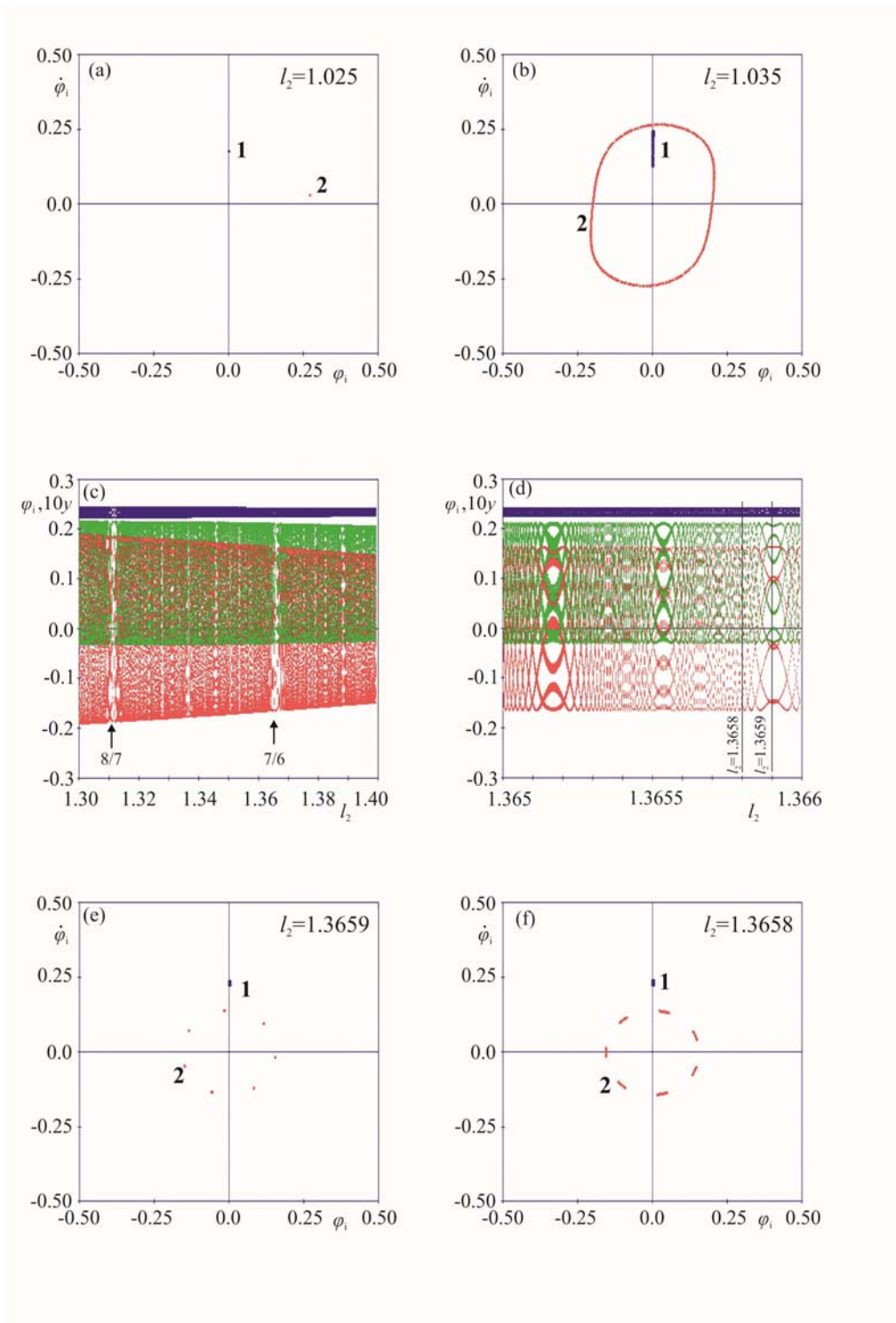


Figure 7. Poincaré maps and bifurcations diagrams of system (3,4) with two nonidentical pendula; (a) Poincaré map for $l_2=1.025$ showing the almost 90° -1-2-synchronization; (b) Poincaré map for $l_2=1.035$ showing the quasi-periodic oscillations; (c) bifurcation diagram with periodic windows; (d) enlargement of the part of bifurcation diagram (c), (e) Poincaré map for $l_2=1.3659$ showing period seven motion; (f) Poincaré map for $l_2=1.3658$, showing quasi-periodic motion.

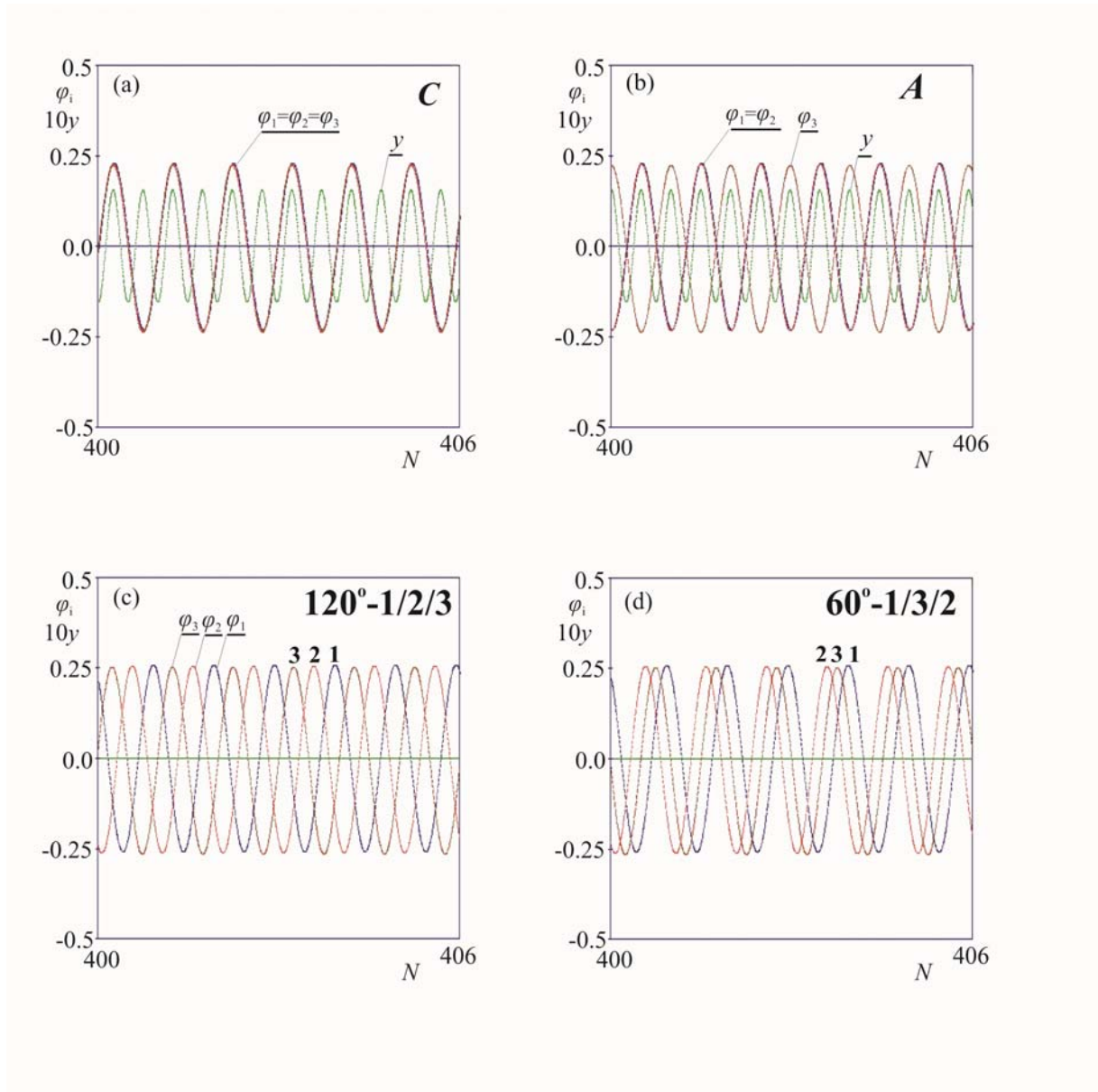


Figure 8. Synchronization system (3,4) with three identical pendula; (a) time series of complete-synchronization (**C**); (b) time series of antiphase-synchronization (**A**); (c) time series of 120° -synchronization; (d) time series of 60° -synchronization.

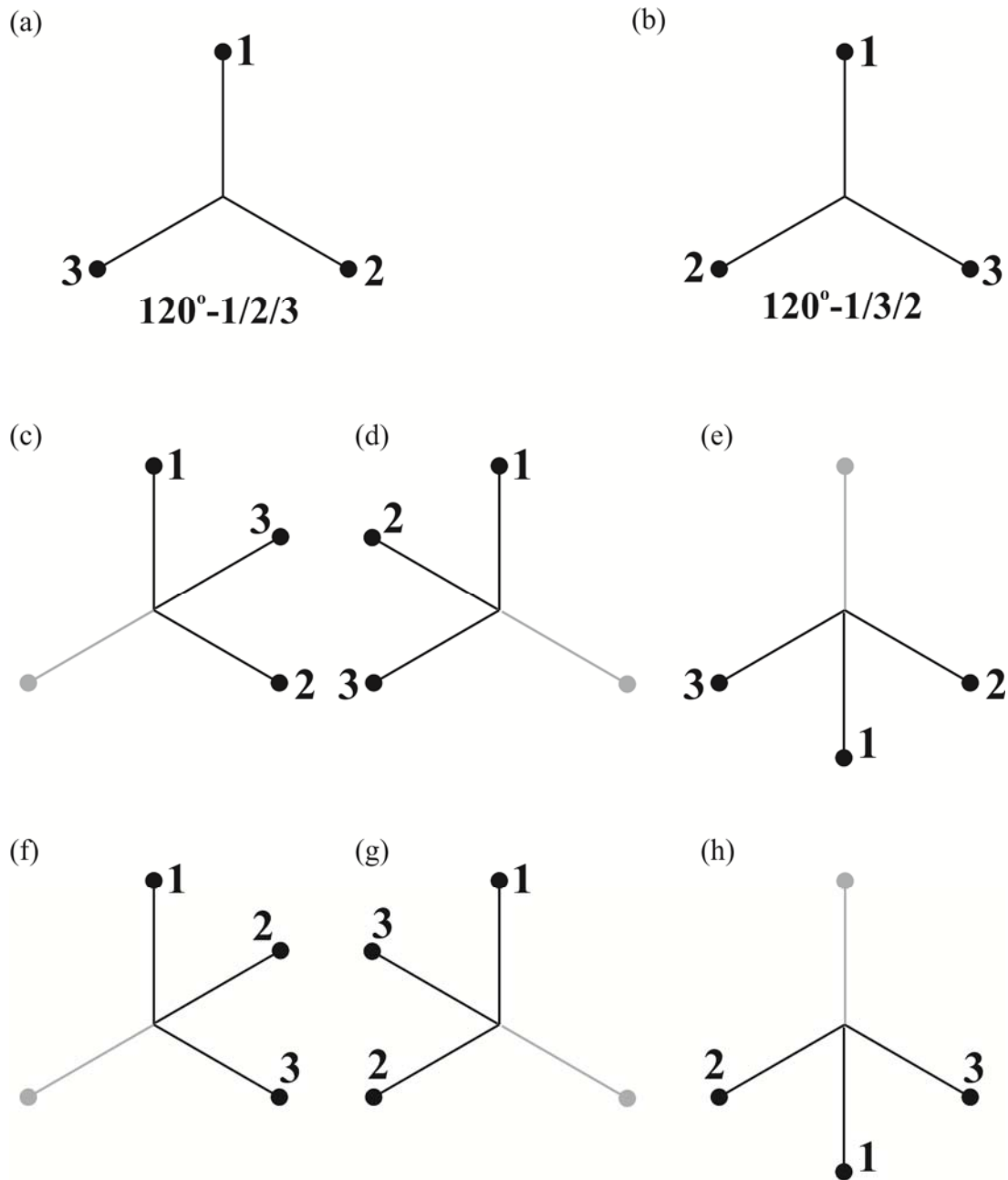


Figure 9. Schemes of 120° - and 60° -synchronizations on the phase plane; (a) 120° -1/2/3-synchronization; (b) 120° -1/3/2-synchronization; (c) 60° -1/3/2-synchronization; (d) 60° -3/2/1-synchronization; (e) 60° -2/1/3-synchronization; (f) 60° -1/2/3-synchronization; (g) 60° -2/3/1-synchronization; (h) 60° -3/1/2-synchronization.

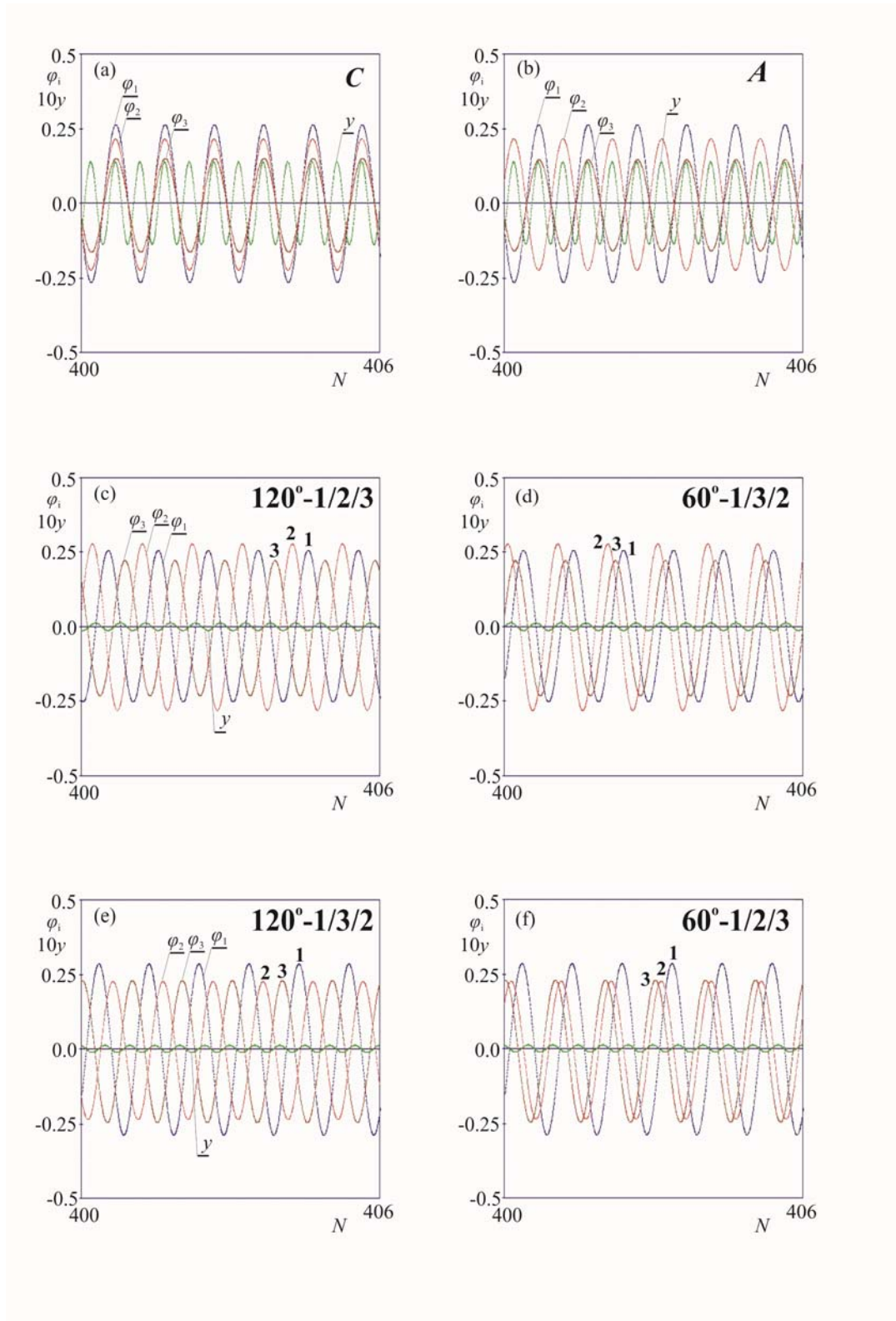


Figure 10. Different types of synchronization in system (3,4) with three pendula: $l_3=1.005$; (a) time series of almost complete-synchronization (C); (b) time series of almost antiphase-synchronization (A); (c) time series of almost 120° -1-2-3-synchronization; (d) time series of almost 60° -1-3-2 synchronization; (e) time series of almost 120° -1-3-2-synchronization; (f) time series of almost 60° -1-2-3- synchronization.

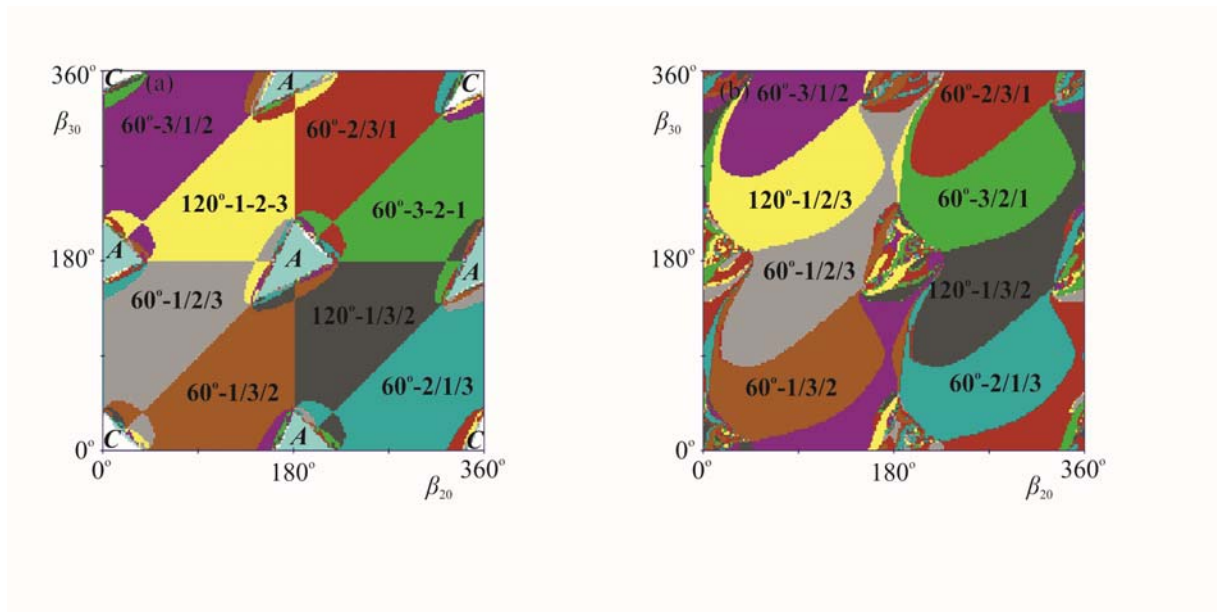


Figure 11. Basins of attraction of various kinds of synchronization; (a) the system with three identical pendulums; (b) the system with three various pendulums, $l_3=1.005$, note that neither almost complete nor almost antiphase synchronization is observed.

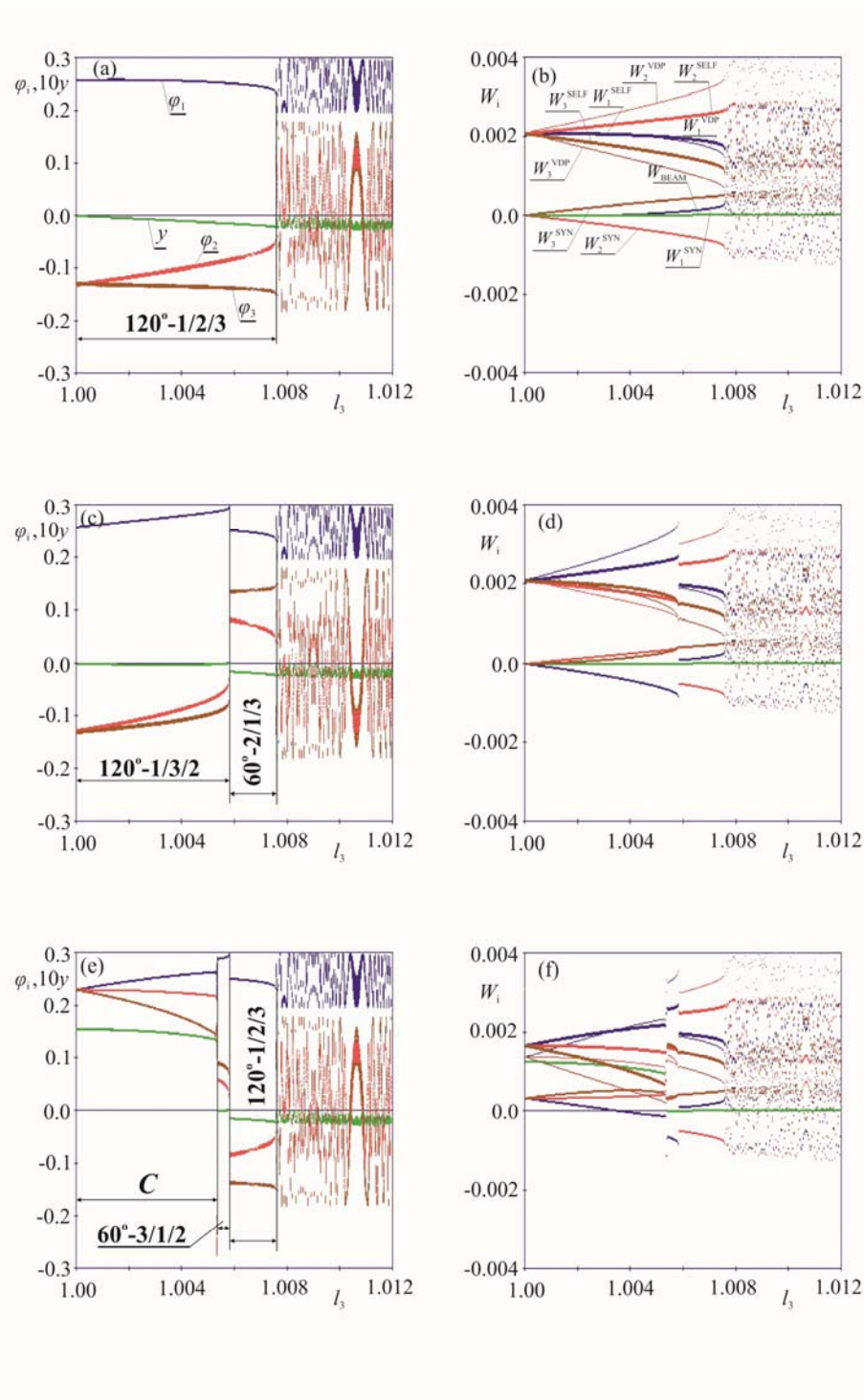


Figure 12. Bifurcation diagrams of the system of three pendula; (a) from 120° -synchronization to quasi-periodic motion – pendula’s displacements; (b) from 120° -synchronization to quasi-periodic motion - energies; (c) from 120° - through almost 60° -synchronization to quasi-periodic motion- displacements; (d) from 120° - through almost 60° -synchronization to quasi-periodic motion- energies; (e) from complete (C) - through almost 60° - and 120° -synchronization to quasi-periodic motion- displacements; (f) from complete- through almost 60° - and 120° -synchronization to quasi-periodic motion- energies.

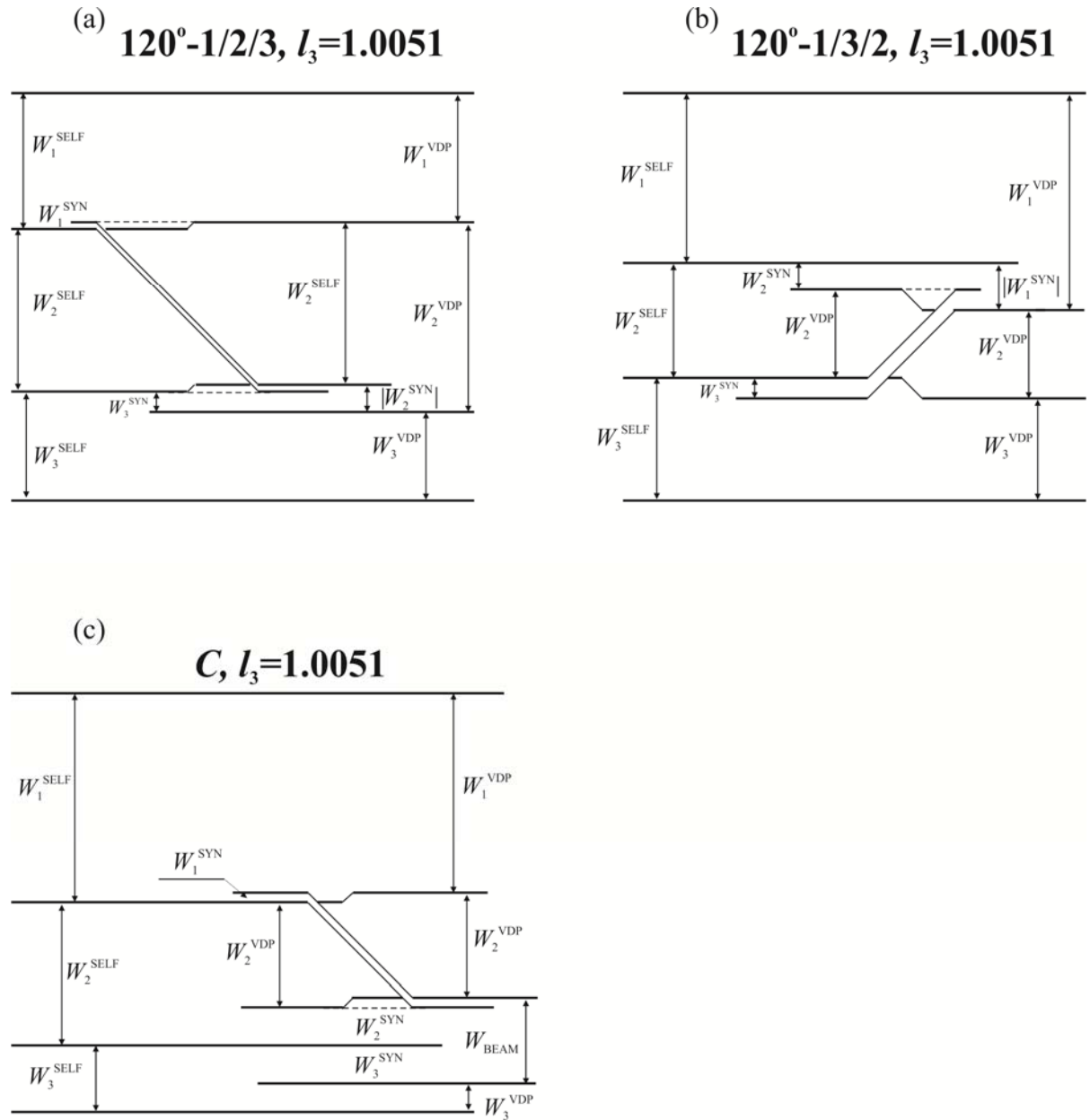


Figure 13. Energy balances of the system (1) for $l_3=1.0051$; (a) almost $120^\circ\text{-}1/2/3$ -synchronization; (b) almost $120^\circ\text{-}1/3/2$ -synchronization; (c) almost complete-synchronization (C).

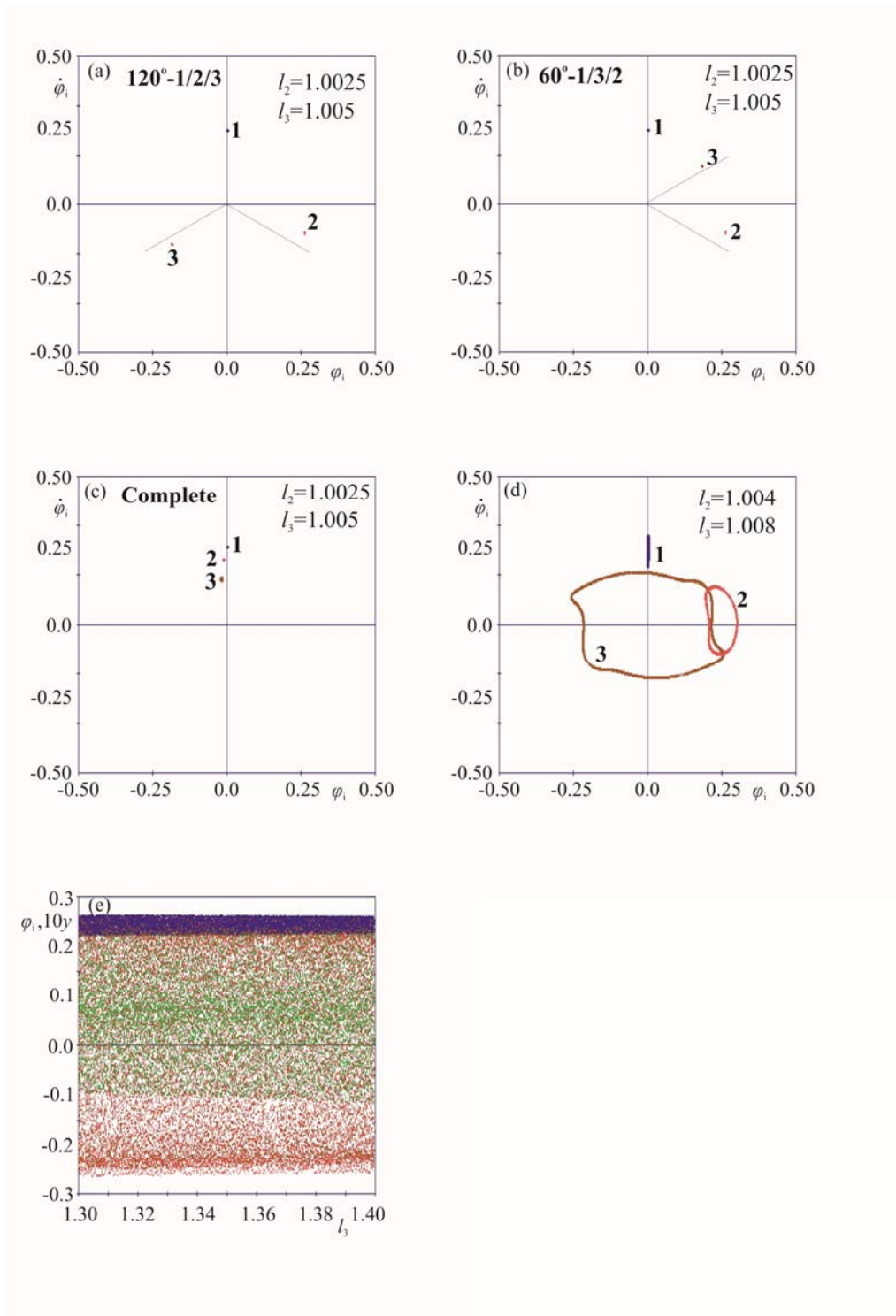


Figure 14. Poincaré maps and bifurcation diagram of the system with three nonidentical pendula; (a) Poincaré map for $l_3=1.005$ showing the almost 120° -1-2-3-synchronization; (b) Poincaré map for $l_3=1.005$ showing the energetically identical almost 60° -1-3-2-synchronization; (c) Poincaré map for $l_3=1.005$, showing the almost complete-synchronization, (d) Poincaré map for $l_3=1.008$, showing quasi-periodic motion, (e) bifurcation diagram without periodic windows.

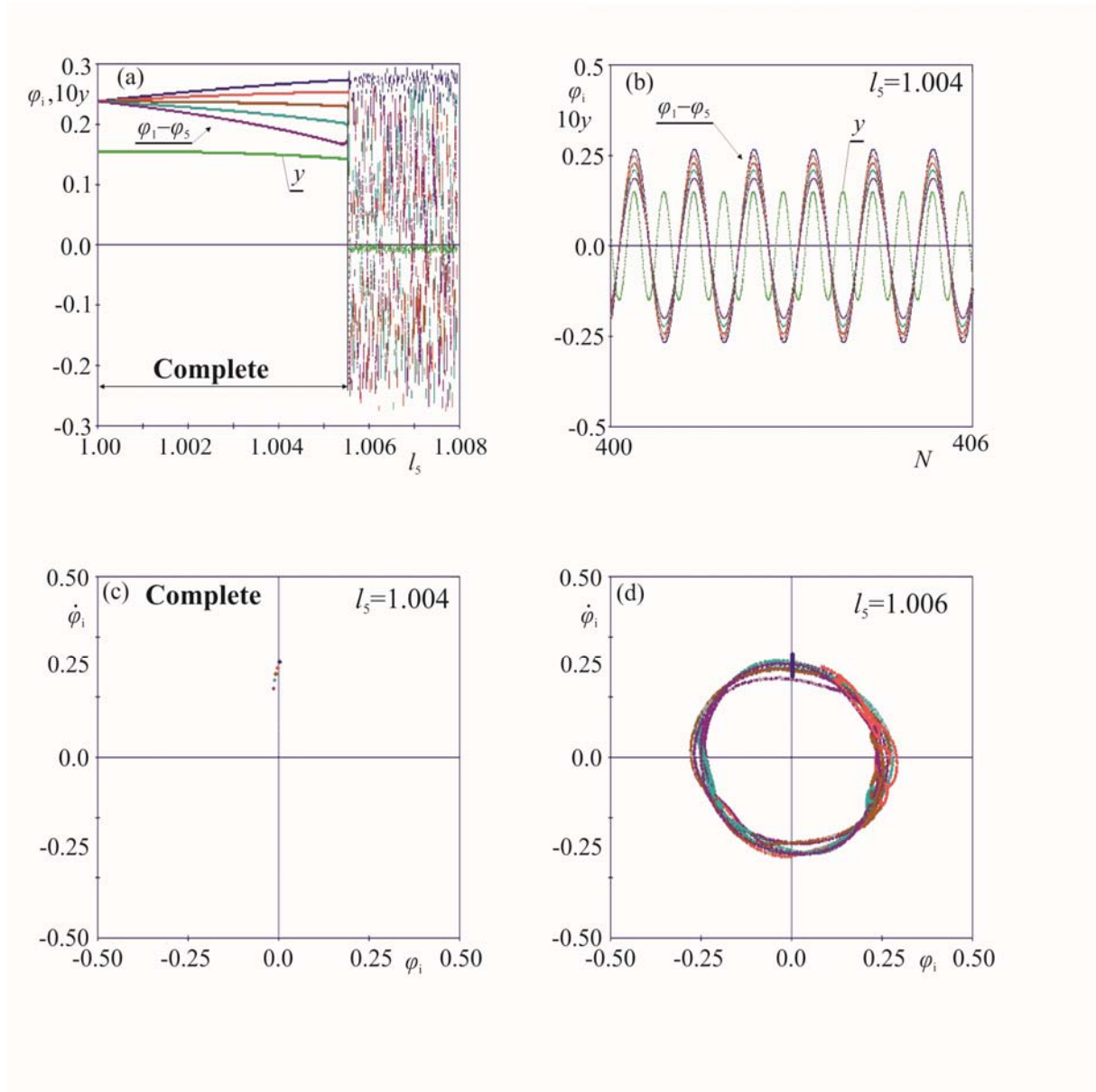


Figure 15. Bifurcations diagram, time series and Poincare maps for the system with five pendula; (a) bifurcation diagram from complete synchronization to quasi-periodic oscillations; (b) time series of almost complete-synchronization for $l_5=1.004$; (c) Poincare map for $l_5=1.004$ showing the almost complete-synchronization; (d) Poincare map for $l_5=1.006$ showing quasi-periodic oscillations.

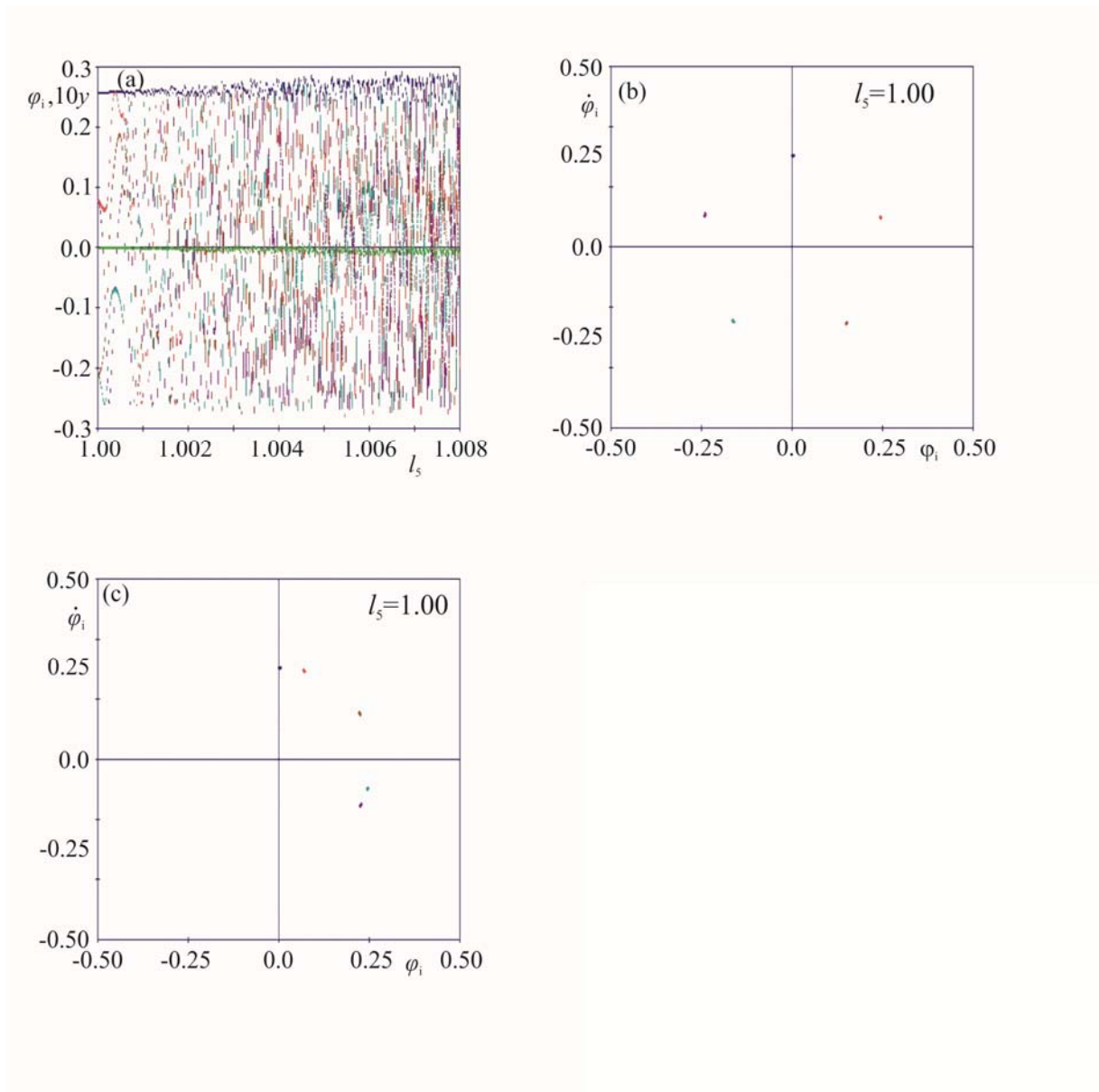


Figure 16. Bifurcation diagram and Poincaré maps for system (3,4) with five nonidentical pendula; (a) bifurcation diagram from phase synchronization to quasi-periodic oscillations; (b) Poincaré map for $l_5=1.0$ showing the phase shifts between the pendula, (c) Poincaré map for $l_5=1.0$ showing the different phase shifts between the pendula.